

Vestigial singlet pairing in a fluctuating magnetic triplet superconductor: Applications to graphene moiré systems

Prathyush P. Poduval¹ and Mathias S. Scheurer²

¹*Condensed Matter Theory Center, Department of Physics,
University of Maryland, College Park, MD 20742, USA*

²*Institute for Theoretical Physics, University of Innsbruck, Innsbruck A-6020, Austria*

Motivated by the phenomenology of graphene moiré superlattices, we study a 2D model with strong tendencies towards both magnetism and triplet superconductivity. Individually, their respective order parameters, \mathbf{N} and \mathbf{d} , cannot order at finite temperature. Nonetheless, the model exhibits a variety of vestigial phases, including charge- $4e$ superconductivity and broken time-reversal symmetry. Our main focus is on a phase characterized by finite $\mathbf{d} \cdot \mathbf{N}$, which has the same symmetries as the BCS state, a Meissner effect, and metastable supercurrents, yet rather different spectral properties: most notably, the suppression of the electronic density of states at the Fermi can resemble that of either a fully gapped or nodal superconductor, depending on parameters. This could provide a possible explanation for recent tunneling experiments in graphene moiré systems.

Strongly correlated systems often exhibit complex phase diagrams with multiple phases, characterized by long-range or quasi-long-range order (QLRO) of different order parameters. Aside from phase competition as a possible origin, a rich set of phases might also be understood as different manifestations of an underlying primary order—a concept often referred to as “intertwined orders” [1]. For instance, thermal or quantum fluctuations can disorder a primary order parameter, while higher-order composite order parameters can still survive. An example of such a “vestigial phase” [2, 3], is the charge- $4e$ superconducting state that emerges when a charge- $2e$ pair density wave order parameter, $\Delta_{\mathbf{Q}}$, itself vanishes, yet $\Delta_{\mathbf{Q}}\Delta_{-\mathbf{Q}}$ does not [4]; this and other forms of charge- $4e$ superconductivity have attracted a lot of attention [5–18], in particular, as a result of recent experiments [19, 20].

Another exciting recent development is the emergence of twisted graphene moiré superlattices as versatile playgrounds for strongly correlated physics [21, 22]. These systems display a variety of different phases such as nematic [23–25] and density-wave order [26–28], different forms of magnetism [29–33], and, possibly unconventional [34, 35], superconductivity [36]; magnetism and superconductivity appear in the same density range [34, 35, 37–41] and recent experiments [33, 42] demonstrate that they can coexist microscopically. Motivated by these observations, we here study the case of two primary order parameters: a fully gapped spin-triplet superconductor (\mathbf{d}) and, in line with the conclusions of [41, 43], magnetic order (\mathbf{N}) with antiparallel spins in the two valleys. At finite temperature, $T > 0$, it must hold $\langle \mathbf{d} \rangle = \langle \mathbf{N} \rangle = 0$, in two-dimensions (2D). However, there are several different vestigial phases, see Fig. 1(a), characterized by the composite order parameters $\phi_{dd} = \mathbf{d} \cdot \mathbf{d}$, $\phi_{dN} = \mathbf{d} \cdot \mathbf{N}$, and $\phi_{ddN} = i(\mathbf{d}^\dagger \times \mathbf{d}) \cdot \mathbf{N}$. These include not only a charge- $4e$ superconductor [44, 45], see Fig. 1(b), but also a charge- $2e$ state, which has the same symme-

tries as and is, hence, adiabatically connected to the BCS state. However, it should primarily be thought as a condensate of three electrons and a hole, see Fig. 1(c), or, more formally, QLRO of ϕ_{dN} . We develop a theory for this state and study its spectral properties at finite T , which are rather different from those of the BCS state. Depending on T and ϕ_{dN} , we obtain a low-energy suppression of the density of states (DOS) similar to a fully gapped or nodal state. This could provide an alternative explanation [43, 46, 47] to the tunneling data of [34, 35], which does not require any momentum dependence in the superconducting order parameter.

Model.—We consider a 2D model exhibiting both triplet superconductivity and magnetism, with three-component order parameter fields \mathbf{d} (complex) and \mathbf{N} (real), respectively. Denoting the electronic field operators of spin $s = \uparrow, \downarrow$ (Pauli matrices \mathbf{s}) and in valley $\tau = \pm$ (Pauli matrices $\boldsymbol{\tau}$) by $c_{k,s,\tau}$, where $k = (i\omega_n, \mathbf{k})$ comprises

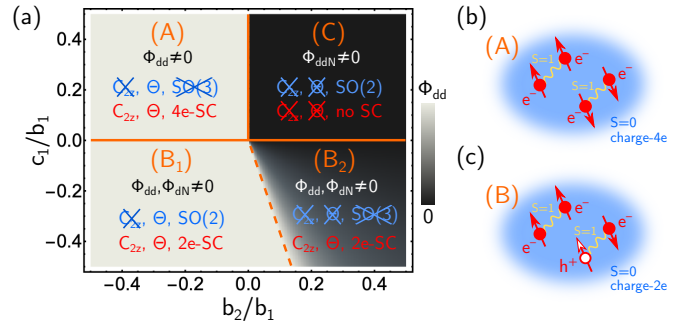


FIG. 1: (a) Mean-field phase diagram for $r_d = r_N$, $b_3 = b_1$, $c_2 = 0$, where we indicate the symmetries at $T = 0$ (blue), and those of the resulting vestigial phases at $T > 0$ (red), and which composite order parameters are finite. Solid (dashed) orange lines are phase transitions at $T = 0$ and $T > 0$ (become a crossover at $T > 0$). (b,c) illustrate the finite- T pairing in phases (A) and (B) schematically.

Matsubara frequencies and 2D momentum, they couple as

$$\mathcal{S}_c = \lambda \int_{k,q} \left[c_{k-q}^\dagger \mathbf{s} \mathbf{N}_q \tau_z c_k + (c_{k-q}^\dagger \mathbf{s} \mathbf{d}_q i s_y \tau_y c_{-k}^\dagger + \text{H.c.}) \right].$$

Note that \mathbf{N} couples anti-ferromagnetically in the two valleys; while the ferromagnetic case—with τ_0 instead of τ_z in the first term of \mathcal{S}_c above—can be studied similarly, we focus on antiferromagnetism not only for concreteness here but also because recent microwave experiments [41] and a systematic analysis [43] of multiple other experiments on graphene moiré systems favor this scenario. The bare dynamics of \mathbf{d} and \mathbf{N} is governed by

$$\mathcal{S}_\chi = \int_q \left[\chi_N^{-1}(q) \mathbf{N}_q \mathbf{N}_{-q} + \chi_d^{-1}(q) \mathbf{d}_q^\dagger \mathbf{d}_q \right].$$

We take the susceptibilities to be $\chi_\mu(q) = \chi_\mu^0 / (r_\mu + \Omega_n^2 + v_\mu^2 q^2)$, $\mu = N, d$, where $q = (i\Omega_n, \mathbf{q})$ and Ω_n are bosonic Matsubara frequencies. The nature of the phase realized in the system depends crucially on the interactions between the bosonic fields. Up to quartic order, the local terms allowed by the symmetries listed in Table I can be written as $\mathcal{S}_V = \int_x V(\mathbf{d}(x), \mathbf{N}(x))$ with

$$V = b_1(\mathbf{d}^\dagger \mathbf{d})^2 + b_2|\mathbf{d}\mathbf{d}|^2 + b_3\mathbf{N}^4 + c_1|\mathbf{d}\mathbf{N}|^2 + c_2(\mathbf{d}^\dagger \mathbf{d})\mathbf{N}^2.$$

Finally, the bare electronic action is given by

$$\mathcal{S}_e = \int_k c_{k,\tau,s}^\dagger (-i\omega_n + \epsilon_{\tau,\mathbf{k}}) c_{k,\tau,s},$$

where we already used that the band structures in the two valleys are related by time-reversal Θ .

Mean-field and possible phases.—To probe the possible phases, we start with a mean-field analysis with respect to \mathbf{d} and \mathbf{N} . Absorbing the impact of the coupling to the electrons [48] by a redefinition of the parameters of V , we obtain the four distinct zero-temperature phases labeled (A), (B_{1,2}), and (C) in Fig. 1(a), where we assumed that both $\langle \mathbf{d} \rangle$ and $\langle \mathbf{N} \rangle$ are non-zero and homogeneous. Using $\hat{e}_{1,2,3} \in \mathbb{R}^3$ to denote orthogonal unit vectors, we have $\mathbf{N} = N_0 \hat{e}_1$ and $\mathbf{d} = d_0 e^{i\alpha} \hat{e}_2$ in phase (A), which breaks SO(3) completely, while Θ is preserved (in any gauge-invariant observable); as for any phase with $\langle \mathbf{N} \rangle \neq 0$, C_{2z} is broken. In phase (B₁), \mathbf{N} and \mathbf{d} are aligned; we, thus, obtain a residual spin-rotation symmetry SO(2) along that direction and Θ is preserved too. Beyond a critical value of b_2 , an additional component with relative phase $\pi/2$ emerges in \mathbf{d} , defining phase (B₂) where $\mathbf{N} = N_0 \hat{e}_1$ and $\mathbf{d} = d_0 e^{i\alpha} (\hat{e}_1 + i\eta \hat{e}_2)$, with $0 < \eta < 1$; this is a distinct phase as $\eta \neq 0$ breaks both the residual SO(2) spin symmetry and Θ . Finally, phase (C) is characterized by $\mathbf{N} = N_0 \hat{e}_1$ and $\mathbf{d} = d_0 e^{i\alpha} (\hat{e}_2 + i\hat{e}_3)$. Consequently, Θ is also broken but a residual SO(2) spin-symmetry remains.

Importantly, $\langle \mathbf{d} \rangle, \langle \mathbf{N} \rangle \neq 0$ is only possible and, thus, our discussion of symmetries is only valid for $T = 0$ in

TABLE I: Relevant symmetries g and their action on the field operators. Here R_φ is the orthogonal matrix obeying $e^{-i\varphi \cdot \mathbf{s}} \mathbf{s} e^{i\varphi \cdot \mathbf{s}} = R(\varphi) \mathbf{s}$. All symmetries are linear except for Θ which is anti-linear.

g	$c_{\mathbf{k}}$	\mathbf{N}	\mathbf{d}	ϕ_{dd}	ϕ_{dN}	ϕ_{ddN}
$U(1)$	$e^{i\varphi} c_{\mathbf{k}}$	\mathbf{N}	$e^{-2i\varphi} \mathbf{d}$	$e^{-4i\varphi} \phi_{dd}$	$e^{-2i\varphi} \phi_{dN}$	ϕ_{ddN}
SO(3)	$e^{i\varphi \cdot \mathbf{s}} c_{\mathbf{k}}$	$R_\varphi \mathbf{N}$	$R_\varphi \mathbf{d}$	ϕ_{dd}	ϕ_{dN}	ϕ_{ddN}
C_{2z}	$\tau_x c_{-\mathbf{k}}$	$-\mathbf{N}$	$-\mathbf{d}$	ϕ_{dd}	ϕ_{dN}	$-\phi_{ddN}$
Θ	$i s_y \tau_x c_{-\mathbf{k}}$	\mathbf{N}	$-\mathbf{d}^*$	ϕ_{dd}^*	$-\phi_{dN}^*$	$-\phi_{ddN}$

2D. To analyze the resulting vestigial phases at finite T , where SO(3) spin-rotation symmetry is preserved and $\langle \mathbf{d} \rangle = \langle \mathbf{N} \rangle = 0$, it is convenient to define the following composite order parameters $\phi_{dd} = \mathbf{d} \cdot \mathbf{d}$, $\phi_{dN} = \mathbf{d} \cdot \mathbf{N}$, and $\phi_{ddN} = i(\mathbf{d}^\dagger \times \mathbf{d}) \cdot \mathbf{N}$, with symmetry properties listed in Table I. Crucially, all of them transform trivially under SO(3) spin-rotations and, hence, can exhibit long-range (in case of the last one) or QLRO (in case of the former two) at finite T . We indicate this in Fig. 1(a) for the different phases. This immediately tells us that, in spite of $\langle \mathbf{d} \rangle = 0$, phase (A) transitions for finite T into state where ϕ_{dd} has QLRO and, thus, constitutes a charge- $4e$ superconductor (as $\phi_{dN} = 0$), which does not break C_{2z} or Θ (as $\phi_{ddN} = 0$); intuitively, one can think of this state as a condensate of four electrons forming a spin-singlet out of two triplets, see Fig. 1(b). At finite T , (B₁) and (B₂) will both preserve all normal-state symmetries and become the same phase, which we denote by (B) in the following. It is characterized by QLRO not only in ϕ_{dd} but also in ϕ_{dN} ; as the latter has charge $2e$, it is a charge- $2e$ superconductor and adiabatically connected to the conventional BCS state. Nonetheless, in our current description, this state should rather be thought of as the condensation of three electrons and a hole, see Fig. 1(c), consisting of a pair of electrons in a triplet state forming a singlet with a spin-1 particle-hole excitation. In fact, we will see below that it exhibits spectral properties rather different from those of the BCS state at finite T . Finally, while phase (C) does not exhibit any vestigial pairing at $T > 0$, it will have long-range order in ϕ_{ddN} and, as such, continues to break both C_{2z} and Θ .

Theory for phase (B).—As $c_1 < 0$ is found when the coefficients in V are computed by integrating out electrons [48], we next focus on phase (B). To obtain an efficient description of this phase that properly captures the preserved SO(3) symmetry at finite temperature, we first decouple the four terms in V using four Hubbard-Stratonovich fields, ψ_d for $\mathbf{d}^\dagger \mathbf{d}$, ψ_N for \mathbf{N}^2 , ϕ_d for $\mathbf{d} \cdot \mathbf{d}$, and ϕ_{dN} for $\mathbf{d} \cdot \mathbf{N}$. We treat them on the saddle-point level, which becomes exact in the limit where the number of components of \mathbf{d} and \mathbf{N} is taken to be infinitely

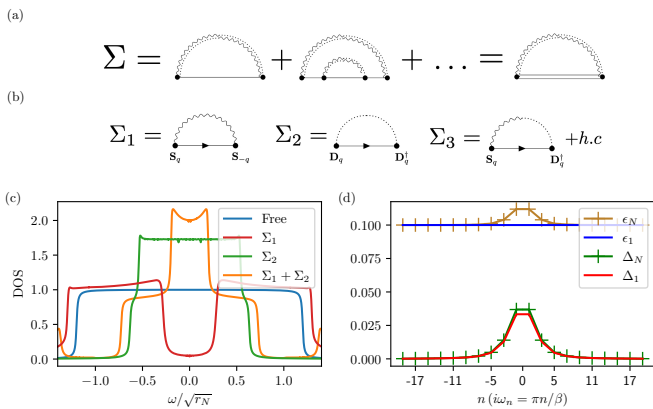


FIG. 2: Diagrams contributing to the fermionic self energy Σ (a) in the matrix-large- N limit defined in the main text and (b) to first order. (c) Impact of spin (Σ_1) and triplet fluctuations (Σ_2) on the constant DOS (blue) of a 2D band with finite bandwidth. (d) Comparing the first order solution (ϵ_1, Δ_1) and self consistent solution (ϵ_N, Δ_N) for $G = i\omega - \epsilon(i\omega)\gamma_z + \Delta(i\omega)\gamma_y$ for \mathcal{S}_2 only (both without momentum integration). We use $\epsilon/\sqrt{r_N} = 0.1, \phi_0/r_N = 0.5$.

large [49]. The saddle point values of ψ_d and ψ_N will in general be non-zero, which we absorb into a redefinition of $r_{d,N}$. Then, the effective action for phase (B) becomes $\mathcal{S}_{\text{eff}} = \mathcal{S}_\chi + \mathcal{S}_e + \mathcal{S}_c + \mathcal{S}_\phi$ where

$$\mathcal{S}_\phi = \int_q [\phi_{dN}^0 \mathbf{d}_q \cdot \mathbf{N}_{-q} + \phi_{dd}^0 \mathbf{d}_q \cdot \mathbf{d}_{-q} + \text{H.c.}]. \quad (1)$$

While generically both saddle point values ϕ_{dN}^0 and ϕ_{dd}^0 are expected to be non-zero simultaneously in phase (B), we take $\phi_{dd}^0 \rightarrow 0$ and $\phi_{dN}^0 \equiv \phi_0 \neq 0$ for the following explicit calculations. Setting $\phi_{dd}^0 = 0$ does not change any symmetries of the phase, and can formally be seen as the large b_2 limit of the theory where ϕ_{dd}^0 is suppressed [cf. Fig. 1(a)]. More generally than the derivation of \mathcal{S}_{eff} via Hubbard-Stratonovich transformations, it can also be thought of as the simplest field theory capturing the key aspects of phase (B) in Fig. 1(a) at finite T .

Electronic self energy.—To compute the spectral properties of the electrons within this model, we employ a large- N technique similar to [50, 51]: we add extra indices to the electrons and bosons, $c_{k,\tau,s} \rightarrow c_{k,\tau,s,a}$, $\mathbf{d}_{ab} \rightarrow \mathbf{d}_{ab}$ and similarly for \mathbf{N} , where $a, b = 1, 2, \dots, N$, which are contracted in all terms of \mathcal{S}_{eff} so as to ensure $O(N)$ symmetry. In the limit $N \rightarrow \infty$, the electronic self-energy Σ is given by the “rainbow diagrams” [50, 51] shown in Fig. 2(a). In our case, however, Σ involves both normal and anomalous contributions as a result of the anomalous bosonic term $\propto \phi_0$ in Eq. (1). To make this more explicit, we integrate out the bosons, yielding the effec-

tive fermionic interactions $\mathcal{S}_{\text{int}} = \mathcal{S}_1 + \mathcal{S}_2$ with

$$\mathcal{S}_1 = - \int_q \frac{\lambda^2}{M_q} \left(\frac{\chi_d^{-1}}{4} \mathbf{S}_q \cdot \mathbf{S}_{-q} + \chi_N^{-1} \mathbf{D}_q \cdot \mathbf{D}_q^\dagger \right), \quad (2a)$$

$$\mathcal{S}_2 = - \frac{1}{2} \int_q \frac{\lambda^2}{M_q} (\phi_0 \mathbf{S}_q \cdot \mathbf{D}_q^\dagger + \phi_0^* \mathbf{D}_q \cdot \mathbf{S}_{-q}), \quad (2b)$$

where $M_q = \chi_d^{-1} \chi_N^{-1} - |\phi_0|^2$ and $\mathbf{S}_q = \int_k c_{k+q}^\dagger \mathbf{s} \tau_z c_k$, $\mathbf{D}_q = \int_k c_{k+q}^\dagger \mathbf{s} i s_y \tau_y c_{-k}^\dagger$. The two terms in \mathcal{S}_1 describe spin and superconducting triplet fluctuations, respectively; their associated self-energy contributions are normal in the sense that $U(1)$ symmetry is preserved, with leading terms represented by the first two diagrams $\Sigma_{1,2}$ in Fig. 2(b). Conversely, \mathcal{S}_2 breaks $U(1)$ symmetry, when ϕ_0 attains a mean-field value, and results in an anomalous contribution to the self-energy, with leading term given by the last diagram Σ_3 in Fig. 2(b).

To represent the diagrams algebraically, we shift to the Bogoliubov-de Gennes basis $(c_{q,+}, i s_y c_{-q,-}^\dagger)^T$, with Pauli matrices γ_i acting on this space. In this basis, the free Green’s function is $G_0(i\omega, \epsilon) = i\omega - \epsilon\gamma_z$. Up to first order in λ^2 , the spin-spin self energy term can be written as $\Sigma_1(k) = 3\lambda^2 \int_q \frac{\chi_d^{-1}(q)}{2M_q} G_0(i\omega + i\Omega, \epsilon_{\mathbf{k}+q})$, while the triplet-triplet term is $\Sigma_2(k) = 12\lambda^2 \int_q \frac{\chi_N^{-1}(q)}{M_q} G_0(i\omega + i\Omega, -\epsilon_{\mathbf{k}+q})$. After performing a gauge transformation to make ϕ_0 real, the anomalous term from the spin-triplet interaction is given by

$$\Sigma_3(k) = 3\phi_0 \int_q \frac{\lambda^2}{M_q} \{\gamma_y, \gamma_z G_0(i\omega + i\Omega, \epsilon_{\mathbf{k}+q})\}. \quad (3)$$

For concreteness and since spin fluctuations are believed to occur already at higher energies than superconducting fluctuations in graphene moiré systems [37, 38], we focus on $r_d > r_N$; we will use $r_d/r_N = 9, v_d^2/v_N^2 = 8, \chi_N^0 = \chi_d^0$, and set $\chi_\mu^0 = 1$ by rescaling of the fields.

Density of states.—Figure 2(c) shows the effect of the normal contributions of the self energy $\Sigma_{1,2}$ on the DOS of a 2D parabolic band. The effect of Σ_1 is to push the peak of the free spectral function at energy ϵ away from $\omega = 0$. This results in the opening of a gap (which can be soft depending on the parameter regime), very similar to fluctuating anti-ferromagnetism discussed in the cuprates [52–54]. Σ_2 on the other hand has the opposite effect, where it pushes states *towards* $\omega = 0$. This is because Σ_1 and Σ_2 have the exact same functional form with one key difference: $\epsilon_{\mathbf{k}+q}$ of Σ_1 is replaced by $-\epsilon_{\mathbf{k}+q}$ in Σ_2 . The effect of the total normal self energy $\Sigma_1 + \Sigma_2$ is to enhance the DOS in the vicinity of the Fermi level, see Fig. 2(c). The anomalous contribution Σ_3 does not interfere in these effects since it occurs in the γ_y channel. The role of $\Sigma_1 + \Sigma_2$ can, thus, be intuitively thought of as providing a renormalized DOS in the normal state on top of which the anomalous Σ_3 opens up

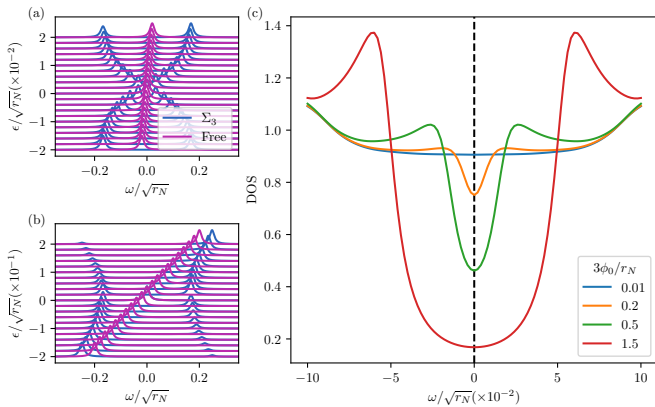


FIG. 3: Spectral weight as a function of ω with (blue) and without (purple) Σ_3 (a) close to $\epsilon_{\mathbf{k}} = 0$ and (b) including a larger energy range; in both cases, we focus on the $\mathbf{q} = 0$ contribution (see text). (c) The effect of all three self energy contributions $\Sigma_1 + \Sigma_2 + \Sigma_3$ (including the momentum integration) on the DOS. For small ϕ_0 , there is suppression of the DOS at $\omega = 0$ which resembles the V-shaped DOS of a nodal state. For large ϕ_0 , the gap resembles a hard BCS gap.

a gap. We have checked [48] by numerically solving the self-consistency equation for the self-energy [Fig. 2(a)] in the limit (of large v_μ) where only the $\mathbf{q} = 0$ term of the momentum sum contributes that higher-order corrections do not change our results qualitatively for small ϕ_0 . For instance, Fig. 2(d) shows the numerical solution for the Green’s function $G = i\omega - \epsilon(i\omega)\gamma_z + \Delta(i\omega)\gamma_y$ in Matsubara space upon including the effect of \mathcal{S}_2 ; the difference to the first-order result is small.

To gain intuition for the impact of Σ_3 on the DOS, we first focus again on the $\mathbf{q} = 0$ term of the momentum sum in Eq. (3). In this limit, one can easily see [48] that Σ_3 vanishes linearly in $\epsilon_{\mathbf{k}}$ for small energies. Since Σ_3 is in the γ_y channel, the effect of any non-zero value is to generically open a gap. As a result of the linear behavior, the states exactly at zero energy are unaffected, but slightly away from it, the states get pushed away to higher energy; this is clearly visible in Fig. 3(a). In contrast, for large energies, Σ_3 is readily seen to tend to zero. The spectral function, thus, remains asymptotically unaffected, as can be seen in Fig. 3(b). Taken together, we expect the DOS to be reduced (but not fully suppressed for small ϕ_0) in an energy range around the Fermi level, exhibiting an enhancement with respect to its normal-state value at intermediate energies, and then approaching the normal-state limit at larger energies.

To demonstrate this explicitly beyond the simple $\mathbf{q} = 0$ limit, we approximate $\epsilon_{\mathbf{k}+\mathbf{q}} \simeq \epsilon_{\mathbf{k}} + v_F q_{\parallel} + \mathbf{q}^2/(2m)$, where q_{\parallel} is the component of \mathbf{q} along \mathbf{k} , and numerically evaluate the momentum integrals to find the total self energy $\Sigma = \Sigma_1 + \Sigma_2 + \Sigma_3$. Choosing $v_F = 1.5v_N$, $2m = \sqrt{r_N}/v_N^2$ for concreteness, Fig. 3(c) shows the resulting DOS. As expected, we see that there is a suppression of the DOS.

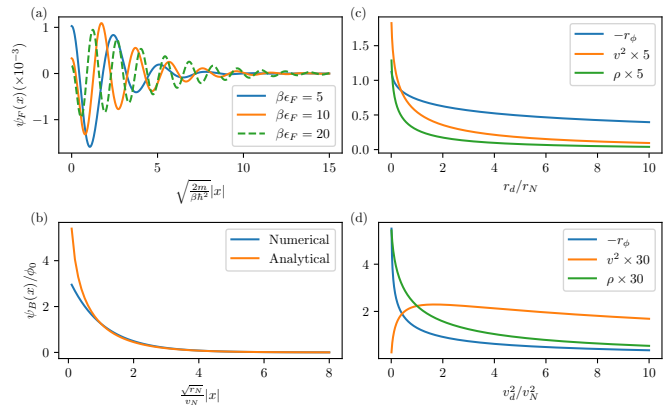


FIG. 4: (a) The fermionic and (b) the bosonic ODLRO “macroscopic wavefunction”. The mass r_ϕ [in units of $r_N^{-1/2}v_N^{-2}$], superfluid density ρ [$r_N^{-3/2}v_N^{-2}$], and velocity v^2 [$r_N^{-3/2}$] of \mathcal{S}_{GL} in Eq. (5) as a function of r_d and v_d^2 are shown in (c) and (d), respectively.

However, for small values of ϕ_0 , the resulting DOS has a V-shaped behavior, which is typically only seen in nodal states (with either nodal lines or points). Recall that the superconducting phase in our model is symmetry-equivalent to a conventional BCS state and that the triplet superconductor that arises at $T = 0$ in phase (B) will be fully gapped. For larger ϕ_0 , the gap at $\omega = 0$ increases, and resembles a hard BCS gap. The suppression of the DOS ρ_F at $\omega = 0$ can be estimated analytically at finite temperature by again taking the limit (of large v_μ) where the integration over \mathbf{q} can be replaced by an evaluation at $\mathbf{q} = 0$; we find

$$\frac{\rho_F(\phi_0)}{\rho_F(\phi_0 = 0)} = \frac{1}{\sqrt{1 + \alpha^2}}, \quad \alpha = \frac{3\phi_0\lambda^2 r_N}{2Tv_N^2(r_d r_N - \phi_0^2)}. \quad (4)$$

Note that ϕ_0^2 is bounded above by $r_d r_N$, at which point the bosonic fields would condense and continuous symmetries would be broken, which cannot happen at finite T . As ϕ_0 increases, α increases the suppression of the DOS, and near the instability point of $\phi_0^2 = r_d r_N$, there are no states near the Fermi surface.

To complement this analysis, we have also studied the Hamiltonian associated with setting $q = 0$ in Eq. (2b) within self-consistent Hartree-Fock, only allowing for spin-rotation invariant operators to condense [48]. For small α , one also finds only a partial suppression of the low-energy spectral weight, akin to Eq. (4); including higher-order corrections leads to a hard gap for $\alpha \geq 1$.

Electromagnetic response.—We will finally demonstrate that the superconducting phase characterized by $\phi_0 \neq 0$ has the same electromagnetic phenomenology as BCS superconductors, despite the unusual electronic spectral properties. To this end, we study off-diagonal long-range order (ODLRO) [55–

[57] which implies the Meissner effect [58], flux quantization [59], Josephson effect and persistent currents [60]. First focusing on the electrons, we show that $\langle c_{s_1,+}^\dagger(\mathbf{x}_1)c_{s_2,-}^\dagger(\mathbf{x}_2)c_{s_2,-}(\mathbf{x}'_2)c_{s_1,+}(\mathbf{x}'_1) \rangle \rightarrow n_0(\Psi_F^*(\mathbf{x}_{12}))_{s_1,s_2}(\Psi_F(\mathbf{x}'_{12}))_{s'_1,s'_2}$, with $\Psi_F \neq 0$, as $|\mathbf{x}_j - \mathbf{x}'_j| \rightarrow \infty$ at finite $\mathbf{x}_{12} = \mathbf{x}_1 - \mathbf{x}_2$ and $\mathbf{x}'_{12} = \mathbf{x}'_1 - \mathbf{x}'_2$, to leading (first) order in ϕ_0 ; as non-zero Ψ_F to linear order in ϕ_0 implies that it cannot vanish identically for generic ϕ_0 , this is sufficient to show the presence of ODLRO. We find the ‘‘macroscopic wave function’’ to be a singlet, $\Psi_F(\mathbf{x}) = is_y\psi_F(\mathbf{x})$, as expected since spin-rotation symmetry is preserved at finite T , with $\psi_F(\mathbf{x})$ shown in Fig. 4(a). Alternatively, one can demonstrate ODLRO to arbitrary order in ϕ_0 , by focusing on the bosons: to zeroth order in λ , we find $\langle (\mathbf{d}^\dagger(\mathbf{x}_1)\mathbf{N}(\mathbf{x}_2))(\mathbf{d}(\mathbf{x}'_1)\mathbf{N}(\mathbf{x}'_2)) \rangle \rightarrow \psi_B^*(\mathbf{x}_{12})\psi_B(\mathbf{x}'_{12})$ as $|\mathbf{x}_j - \mathbf{x}'_j| \rightarrow \infty$, with $\psi_B(\mathbf{x})$ plotted in Fig. 4(b) along with an analytic asymptotic form for large \mathbf{x} ; in [48], we show that this leads to the same constraints as the conventional form of bosonic ODLRO [55, 56]. Finally, the connection to the textbook theory of superconductivity can be made more explicit by deriving the analogue of the time-dependent Ginzburg-Landau theory: we reinstate fluctuations via $\phi_0 \rightarrow \phi(\mathbf{x}, \tau)$ and integrate out all other degrees of freedom yielding

$$\mathcal{S}_{\text{GL}} = \int_{\mathbf{x}, \tau} [\rho |D_\tau \phi|^2 + (r_\phi + |c_1|^{-1})|\phi|^2 + v^2 |\mathbf{D}\phi|^2] \quad (5)$$

to leading order in ϕ and gauge-covariant derivatives $(D_\tau, \mathbf{D})_\mu = \partial_\mu - ieA_\mu$. For demonstration purposes, we evaluated the coefficients in \mathcal{S}_{GL} to leading (zeroth)

order in \mathcal{S}_c and find $\rho, v_\phi > 0$ and $r_\phi < 0$ for low T [see Fig. 4(c,d)]; the state with QLRO in ϕ_0 thus corresponds, as usual, to the Higgs phase, with Meissner effect and massive Higgs mode, but without Goldstone modes.

Conclusion.—We have studied the finite- T vestigial phases, see Fig. 1(a), associated with two primary order parameters, \mathbf{d} and \mathbf{N} , describing a fully gapped triplet superconductor and spin magnetism, respectively. A crucial result is the DOS of phase $(B_{1,2})$ in Fig. 3(c): varying ϕ_0 changes the low-energy DOS from partial suppression, akin to that of a nodal superconducting state, to a hard gap. As ϕ_0 is expected to change with electron filling, this could explain the tunneling data in [34, 35]. We finally point out that the suppression of \mathbf{N} would immediately also suppress ϕ_0 in our model and could, therefore, explain why superconductivity is connected to the reset behavior in trilayer graphene [34, 35, 39, 40].

Acknowledgments. We thank Rafael Fernandes, Victor Gurarie, Peter Orth, and Subir Sachdev for fruitful discussions on the project and Jakob Wessling for a related collaboration. M.S.S. acknowledges funding by the European Union (ERC-2021-STG, Project 101040651—SuperCorr). Views and opinions expressed are however those of the authors only and do not necessarily reflect those of the European Union or the European Research Council Executive Agency. Neither the European Union nor the granting authority can be held responsible for them. P³ acknowledges support by the Laboratory for Physical Sciences through the Condensed Matter Theory Center.

-
- [1] E. Fradkin, S. A. Kivelson, and J. M. Tranquada, ‘‘Colloquium: Theory of intertwined orders in high temperature superconductors,’’ *Reviews of Modern Physics* **87**, 457 (2015).
- [2] L. Nie, G. Tarjus, and S. A. Kivelson, ‘‘Quenched disorder and vestigial nematicity in the pseudogap regime of the cuprates,’’ *Proceedings of the National Academy of Sciences* **111**, 7980 (2014).
- [3] R. M. Fernandes, P. P. Orth, and J. Schmalian, ‘‘Intertwined Vestigial Order in Quantum Materials: Nematicity and Beyond,’’ *Annual Review of Condensed Matter Physics* **10**, 133 (2019).
- [4] E. Berg, E. Fradkin, and S. A. Kivelson, ‘‘Charge-4e superconductivity from pair-density-wave order in certain high-temperature superconductors,’’ *Nature Physics* **5**, 830 (2009).
- [5] R. M. Fernandes and L. Fu, ‘‘Charge- 4 e Superconductivity from Multicomponent Nematic Pairing: Application to Twisted Bilayer Graphene,’’ *Physical Review Letters* **127**, 047001 (2021).
- [6] S.-K. Jian, Y. Huang, and H. Yao, ‘‘Charge- 4 e Superconductivity from Nematic Superconductors in Two and Three Dimensions,’’ *Physical Review Letters* **127**, 227001 (2021).
- [7] M. Zeng, L.-H. Hu, H.-Y. Hu, Y.-Z. You, and C. Wu, ‘‘Phase-fluctuation Induced Time-Reversal Symmetry Breaking Normal State,’’ (2021), [arXiv:2102.06158 \[cond-mat\]](https://arxiv.org/abs/2102.06158).
- [8] F.-F. Song and G.-M. Zhang, ‘‘Phase Coherence of Pairs of Cooper Pairs as Quasi-Long-Range Order of Half-Vortex Pairs in a Two-Dimensional Bilayer System,’’ *Physical Review Letters* **128**, 195301 (2022).
- [9] I. Maccari, J. Carlström, and E. Babaev, ‘‘Possible time-reversal-symmetry-breaking fermionic quadrupling condensate in twisted bilayer graphene,’’ (2022), [arXiv:2206.02698 \[cond-mat\]](https://arxiv.org/abs/2206.02698).
- [10] S. B. Chung and S. K. Kim, ‘‘Berezinskii-Kosterlitz-Thouless transition transport in spin-triplet superconductor,’’ *SciPost Physics Core* **5**, 003 (2022).
- [11] Y.-F. Jiang, Z.-X. Li, S. A. Kivelson, and H. Yao, ‘‘Charge-4e superconductors: A Majorana quantum Monte Carlo study,’’ *Physical Review B* **95**, 241103 (2017).
- [12] P. Li, K. Jiang, and J. Hu, ‘‘Charge 4e superconductor:

- A wavefunction approach,” (2022), [arXiv:2209.13905 \[cond-mat\]](#).
- [13] N. V. Gnezdilov and Y. Wang, “Solvable model for a charge-4e superconductor,” *Physical Review B* **106**, 094508 (2022).
- [14] J. B. Curtis, N. R. Poniatowski, Y. Xie, A. Yacoby, E. Demler, and P. Narang, “Stabilizing fluctuating spin-triplet superconductivity in graphene via induced spin-orbit coupling,” (2022), [arXiv:2209.10560 \[cond-mat\]](#).
- [15] J. Garaud and E. Babaev, “Effective Model and Magnetic Properties of the Resistive Electron Quadrupling State,” *Physical Review Letters* **129**, 087602 (2022).
- [16] Z. Pan, C. Lu, F. Yang, and C. Wu, “Frustrated superconductivity and “charge-6e” ordering,” (2022), [arXiv:2209.13745 \[cond-mat\]](#).
- [17] Y. Yu, “Non-uniform vestigial charge-4e phase in the Kagome superconductor CsV_3Sb_5 ,” (2022), [arXiv:2210.00023 \[cond-mat\]](#).
- [18] S. Zhou and Z. Wang, “Chern Fermi pocket, topological pair density wave, and charge-4e and charge-6e superconductivity in kagomé superconductors,” *Nature Communications* **13**, 7288 (2022).
- [19] V. Grinenko, D. Weston, F. Caglieris, C. Wuttke, C. Hess, T. Gottschall, I. Maccari, D. Gorbunov, S. Zherlitsyn, J. Wosnitzer, A. Rydh, K. Kihou, C.-H. Lee, R. Sarkar, S. Dengre, J. Garaud, A. Charnukha, R. Hühne, K. Nielsch, B. Büchner, H.-H. Klauss, and E. Babaev, “State with spontaneously broken time-reversal symmetry above the superconducting phase transition,” *Nature Physics* **17**, 1254 (2021).
- [20] J. Ge, P. Wang, Y. Xing, Q. Yin, H. Lei, Z. Wang, and J. Wang, “Discovery of charge-4e and charge-6e superconductivity in kagome superconductor CsV_3Sb_5 ,” (2022), [arXiv:2201.10352 \[cond-mat\]](#).
- [21] E. Y. Andrei and A. H. MacDonald, “Graphene bilayers with a twist,” *Nature Materials* **19**, 1265 (2020).
- [22] L. Balents, C. R. Dean, D. K. Efetov, and A. F. Young, “Superconductivity and strong correlations in moiré flat bands,” *Nature Physics* **16**, 725 (2020).
- [23] A. Kerelsky, L. J. McGilly, D. M. Kennes, L. Xian, M. Yankowitz, S. Chen, K. Watanabe, T. Taniguchi, J. Hone, C. Dean, A. Rubio, and A. N. Pasupathy, “Maximized electron interactions at the magic angle in twisted bilayer graphene,” *Nature* **572**, 95 (2019).
- [24] Y. Cao, D. Rodan-Legrain, J. M. Park, N. F. Q. Yuan, K. Watanabe, T. Taniguchi, R. M. Fernandes, L. Fu, and P. Jarillo-Herrero, “Nematicity and competing orders in superconducting magic-angle graphene,” *Science* **372**, 264 (2021).
- [25] C. Rubio-Verdú, S. Turkel, Y. Song, L. Klebl, R. Samajdar, M. S. Scheurer, J. W. F. Venderbos, K. Watanabe, T. Taniguchi, H. Ochoa, L. Xian, D. M. Kennes, R. M. Fernandes, Á. Rubio, and A. N. Pasupathy, “Moiré nematic phase in twisted double bilayer graphene,” *Nature Physics* **18**, 196 (2022).
- [26] M. He, J. Cai, Y.-H. Zhang, Y. Liu, Y. Li, T. Taniguchi, K. Watanabe, D. H. Cobden, M. Yankowitz, and X. Xu, “Chirality-dependent topological states in twisted double bilayer graphene,” (2021), [arXiv:2109.08255 \[cond-mat\]](#).
- [27] H. Polshyn, Y. Zhang, M. A. Kumar, T. Soejima, P. Ledwith, K. Watanabe, T. Taniguchi, A. Vishwanath, M. P. Zaletel, and A. F. Young, “Topological charge density waves at half-integer filling of a moiré superlattice,” *Nature Physics* **18**, 42 (2022).
- [28] P. Siriviboon, J.-X. Lin, X. Liu, H. D. Scammell, S. Liu, D. Rhodes, K. Watanabe, T. Taniguchi, J. Hone, M. S. Scheurer, and J. I. A. Li, “A new flavor of correlation and superconductivity in small twist-angle trilayer graphene,” (2022), [arXiv:2112.07127 \[cond-mat\]](#).
- [29] A. L. Sharpe, E. J. Fox, A. W. Barnard, J. Finney, K. Watanabe, T. Taniguchi, M. A. Kastner, and D. Goldhaber-Gordon, “Emergent ferromagnetism near three-quarters filling in twisted bilayer graphene,” *Science* **365**, 605 (2019).
- [30] H. Polshyn, J. Zhu, M. A. Kumar, Y. Zhang, F. Yang, C. L. Tschirhart, M. Serlin, K. Watanabe, T. Taniguchi, A. H. MacDonald, and A. F. Young, “Electrical switching of magnetic order in an orbital Chern insulator,” *Nature* **588**, 66 (2020).
- [31] S. Chen, M. He, Y.-H. Zhang, V. Hsieh, Z. Fei, K. Watanabe, T. Taniguchi, D. H. Cobden, X. Xu, C. R. Dean, and M. Yankowitz, “Electrically tunable correlated and topological states in twisted monolayer-bilayer graphene,” *Nature Physics* **17**, 374 (2021).
- [32] M. Kuri, C. Coleman, Z. Gao, A. Vishnuradhan, K. Watanabe, T. Taniguchi, J. Zhu, A. H. MacDonald, and J. Folk, “Spontaneous time-reversal symmetry breaking in twisted double bilayer graphene,” *Nature Communications* **13**, 6468 (2022), [arXiv:2204.03442 \[cond-mat\]](#).
- [33] J.-X. Lin, P. Siriviboon, H. D. Scammell, S. Liu, D. Rhodes, K. Watanabe, T. Taniguchi, J. Hone, M. S. Scheurer, and J. I. A. Li, “Zero-field superconducting diode effect in small-twist-angle trilayer graphene,” *Nature Physics* **18**, 1221 (2022).
- [34] H. Kim, Y. Choi, C. Lewandowski, A. Thomson, Y. Zhang, R. Polski, K. Watanabe, T. Taniguchi, J. Alicea, and S. Nadj-Perge, “Evidence for unconventional superconductivity in twisted trilayer graphene,” *Nature* **606**, 494 (2022).
- [35] M. Oh, K. P. Nuckolls, D. Wong, R. L. Lee, X. Liu, K. Watanabe, T. Taniguchi, and A. Yazdani, “Evidence for unconventional superconductivity in twisted bilayer graphene,” *Nature* **600**, 240 (2021).
- [36] Y. Cao, V. Fatemi, S. Fang, K. Watanabe, T. Taniguchi, E. Kaxiras, and P. Jarillo-Herrero, “Unconventional superconductivity in magic-angle graphene superlattices,” *Nature* **556**, 43 (2018).
- [37] D. Wong, K. P. Nuckolls, M. Oh, B. Lian, Y. Xie, S. Jeon, K. Watanabe, T. Taniguchi, B. A. Bernevig, and A. Yazdani, “Cascade of electronic transitions in magic-angle twisted bilayer graphene,” *Nature* **582**, 198 (2020).
- [38] U. Zondiner, A. Rozen, D. Rodan-Legrain, Y. Cao, R. Queiroz, T. Taniguchi, K. Watanabe, Y. Oreg, F. von Oppen, A. Stern, E. Berg, P. Jarillo-Herrero, and S. Ilani, “Cascade of phase transitions and Dirac revivals in magic-angle graphene,” *Nature* **582**, 203 (2020).
- [39] J. M. Park, Y. Cao, K. Watanabe, T. Taniguchi, and P. Jarillo-Herrero, “Tunable strongly coupled superconductivity in magic-angle twisted trilayer graphene,” *Nature* **590**, 249 (2021).
- [40] Z. Hao, A. M. Zimmerman, P. Ledwith, E. Khalaf, D. H. Najafabadi, K. Watanabe, T. Taniguchi, A. Vishwanath,

- and P. Kim, “Electric field-tunable superconductivity in alternating-twist magic-angle trilayer graphene,” *Science* **371**, 1133 (2021).
- [41] E. Morissette, J.-X. Lin, D. Sun, L. Zhang, S. Liu, D. Rhodes, K. Watanabe, T. Taniguchi, J. Hone, J. Polaneni, M. S. Scheurer, M. Lilly, A. Mounce, and J. I. A. Li, “[Electron spin resonance and collective excitations in magic-angle twisted bilayer graphene](#),” (2022), [arXiv:2206.08354 \[cond-mat\]](#).
- [42] H. D. Scammell, J. I. A. Li, and M. S. Scheurer, “Theory of zero-field superconducting diode effect in twisted trilayer graphene,” *2D Materials* **9**, 025027 (2022).
- [43] E. Lake, A. S. Patri, and T. Senthil, “Pairing symmetry of twisted bilayer graphene: A phenomenological synthesis,” *Physical Review B* **106**, 104506 (2022).
- [44] C. Xu and L. Balents, “Topological Superconductivity in Twisted Multilayer Graphene,” *Physical Review Letters* **121**, 087001 (2018).
- [45] M. S. Scheurer and R. Samajdar, “Pairing in graphene-based moiré superlattices,” *Physical Review Research* **2**, 033062 (2020).
- [46] P. O. Sukhachov, F. von Oppen, and L. I. Glazman, “Andreev reflection in scanning tunneling spectroscopy of unconventional superconductors,” (2022), [arXiv:2208.05979 \[cond-mat\]](#).
- [47] S. F. Islam, A. Y. Zyuzin, and A. A. Zyuzin, “[Unconventional superconductivity with preformed pairs in twisted bilayer graphene](#),” (2022), [arXiv:2208.12039 \[cond-mat\]](#).
- [48] See Appendix.
- [49] R. M. Fernandes, A. V. Chubukov, J. Knolle, I. Eremin, and J. Schmalian, “Preemptive nematic order, pseudogap, and orbital order in the iron pnictides,” *Physical Review B* **85**, 024534 (2012).
- [50] A. L. Fitzpatrick, S. Kachru, J. Kaplan, and S. Raghu, “Non-Fermi-liquid behavior of large- N B quantum critical metals,” *Physical Review B* **89**, 165114 (2014).
- [51] Y. Werman and E. Berg, “Mott-Ioffe-Regel limit and resistivity crossover in a tractable electron-phonon model,” *Physical Review B* **93**, 075109 (2016).
- [52] B. Kyung, V. Hankevych, A.-M. Daré, and A.-M. S. Tremblay, “Pseudogap and Spin Fluctuations in the Normal State of the Electron-Doped Cuprates,” *Physical Review Letters* **93**, 147004 (2004).
- [53] Y. M. Vilk and A.-M. S. Tremblay, “Non-Perturbative Many-Body Approach to the Hubbard Model and Single-Particle Pseudogap,” *Journal de Physique I* **7**, 1309 (1997).
- [54] M. S. Scheurer, S. Chatterjee, W. Wu, M. Ferrero, A. Georges, and S. Sachdev, “Topological order in the pseudogap metal,” *Proceedings of the National Academy of Sciences* **115**, E3665 (2018).
- [55] O. Penrose and L. Onsager, “Bose-Einstein Condensation and Liquid Helium,” *Physical Review* **104**, 576 (1956).
- [56] O. Penrose, “CXXXVI. On the quantum mechanics of helium II,” *The London, Edinburgh, and Dublin Philosophical Magazine and Journal of Science* **42**, 1373 (1951).
- [57] C. N. Yang, “Concept of Off-Diagonal Long-Range Order and the Quantum Phases of Liquid He and of Superconductors,” *Reviews of Modern Physics* **34**, 694 (1962).
- [58] G. L. Sewell, “Off-diagonal long-range order and the Meissner effect,” *Journal of Statistical Physics* **61**, 415 (1990).
- [59] H. T. Nieh, G. Su, and B.-H. Zhao, “Off-diagonal long-range order: Meissner effect and flux quantization,” *Physical Review B* **51**, 3760 (1995).
- [60] G. L. Sewell, “Off-diagonal long range order and superconductive electrodynamics,” *Journal of Mathematical Physics* **38**, 2053 (1997).
- [61] R. M. Fernandes and A. J. Millis, “Nematicity as a Probe of Superconducting Pairing in Iron-Based Superconductors,” *Physical Review Letters* **111**, 127001 (2013).
- [62] V. Kozii, H. Isobe, J. W. F. Venderbos, and L. Fu, “Nematic superconductivity stabilized by density wave fluctuations: Possible application to twisted bilayer graphene,” *Physical Review B* **99**, 144507 (2019).

Appendix A: Mean-field form of the bosonic interactions

In the main text, we view the field theory defined by the action $\mathcal{S} = \mathcal{S}_e + \mathcal{S}_\chi + \mathcal{S}_c + \mathcal{S}_V$ as an effective low-energy theory that arises when high-energy electronic degrees of freedom have already been integrated out. Due to the symmetry and locality constraints, it only depends on a few parameters, r_μ , v_μ , $b_{1,2,3}$, $c_{1,2}$. As can be seen in Fig. 1(a), in particular, (the sign of) the parameters c_1 and b_2 entering V crucially determine the phase of the system. We here provide an estimate for these parameters using mean-field theory. To this end, we replace the bosonic fields by classical homogeneous and time-independent vectors, $\mathbf{N}_q \rightarrow \delta_{q,0}\mathbf{N}$, $\mathbf{d}_q \rightarrow \delta_{q,0}\mathbf{d}$, in $\mathcal{S}_e + \mathcal{S}_\chi + \mathcal{S}_c$; this yields

$$\mathcal{S}_{\text{HE}} = \int_k c_{k,\tau,s}^\dagger (-i\omega_n + \epsilon_{\tau,\mathbf{k}}) c_{k,\tau,s} + \lambda \int_k \left[c_k^\dagger \mathbf{s} \cdot \mathbf{N} \tau_z c_k + (c_k^\dagger \mathbf{s} \cdot \mathbf{d} i s_y \tau_y c_{-k}^\dagger + \text{H.c.}) \right] + \text{const.}, \quad (\text{A1})$$

which we now view as our full action, also containing the high-energy degrees of freedom. Integrating out the electronic degrees of freedom and expanding the resulting action in terms of \mathbf{N} and \mathbf{d} to quartic order, one obtains exactly the same terms as in V defined in the main text, as expected by symmetry. Moreover, one finds

$$c_1 = b_2 = -b_1/2 < 0, \quad \text{with} \quad b_1 = 32 \lambda^4 T \sum_{\omega_n} \int \frac{d^2 \mathbf{k}}{(2\pi)^2} \frac{1}{(\omega_n^2 + \epsilon_{\mathbf{k}}^2)^2} > 0. \quad (\text{A2})$$

As stated in the main text, this places us into phase (B). We note, however, that fluctuation corrections to mean field can modify the values of these coupling constants significantly [45, 61, 62]. For instance, ferromagnetic fluctuations

can change the sign of b_2 to positive values [45].

Appendix B: Evaluation of the self-energies at leading order

In this section, we show the evaluation of the self energies up to first order in perturbation theory. We first evaluate the anomalous part of the self energy, Σ_3 in Fig. 2(b), which is contributed by the anomalous term of the action given by

$$\mathcal{S}_2 = -\frac{1}{2} \int_q \frac{\lambda^2}{\chi_d^{-1} \chi_N^{-1} - |\phi_0|^2} (\phi_0 \mathbf{S}_q \cdot \mathbf{D}_q^\dagger + \phi_0^* \mathbf{D}_q \cdot \mathbf{S}_{-q}). \quad (\text{B1})$$

In the following, we work in the $(c_{q,+} \quad i s_y c_{-q,-}^\dagger)^T$ Bogoliubov-de Gennes basis, with the Pauli matrices γ_i acting on it. The free Green's function then reads as $G_0^{-1}(k) = i\omega - \epsilon_{\mathbf{k}} \gamma_z$. Choosing ϕ_0 to be real, we have

$$\Sigma_3 = 3 \int_q \frac{\phi_0 \lambda^2}{M_q} (\gamma_y G_{0,k+q} \gamma_z + \gamma_z G_{0,k+q} \gamma_y) = 6 \int_q \frac{\phi_0 \lambda^2}{M_q} \frac{\epsilon_{\mathbf{k}+\mathbf{q}}}{(i\omega + i\Omega)^2 - \epsilon_{\mathbf{k}+\mathbf{q}}^2} \gamma_y, \quad (\text{B2})$$

where

$$M_q = \chi_N^{-1} \chi_d^{-1} - \phi_0^2 = \left(-(i\Omega)^2 + r_N + v_N^2 \mathbf{q}^2 \right) \left(-(i\Omega)^2 + r_d + v_d^2 \mathbf{q}^2 \right) - \phi_0^2 \quad (\text{B3})$$

$$= ((i\Omega)^2 - E_+^2)((i\Omega)^2 - E_-^2), \quad (\text{B4})$$

with $E_\pm^2 = \frac{g_d + g_N \pm \sqrt{(g_d - g_N)^2 + 4\phi_0^2}}{2}$, and $g_\mu = r_\mu + v_\mu^2 \mathbf{q}^2$. Thus,

$$\Sigma_3 = 6\phi_0 \lambda^2 \int_q^T \sum_{i\Omega \in \text{Bosonic}} \frac{1}{\left((i\Omega)^2 - E_+(\mathbf{q})^2 \right) \left((i\Omega)^2 - E_-(\mathbf{q})^2 \right)} \frac{\epsilon_{\mathbf{k}+\mathbf{q}}}{(i\omega + i\Omega)^2 - \epsilon_{\mathbf{k}+\mathbf{q}}^2} \gamma_y. \quad (\text{B5})$$

The Matsubara sum can be evaluated using

$$f(i\omega, \epsilon) = T \sum_{i\Omega} \frac{1}{((i\Omega)^2 - E_+^2)((i\Omega)^2 - E_-^2)} \frac{1}{i\omega + i\Omega - \epsilon} \quad (\text{B6})$$

$$= \frac{1}{2} \frac{1}{E_+^2 - E_-^2} \left(\frac{1}{E_+} (K(i\omega, \epsilon, E_+) - K(i\omega, \epsilon, -E_+)) - \frac{1}{E_-} (K(i\omega, \epsilon, E_-) - K(i\omega, \epsilon, -E_-)) \right), \quad (\text{B7})$$

$$K(i\omega, \epsilon, E) = \frac{n_f(\epsilon) + n_B(-E)}{E + \epsilon - i\omega}, \quad (\text{B8})$$

where $n_{f/B}(\epsilon) = \frac{1}{e^{\beta\epsilon} \pm 1}$. Thus we get,

$$\Sigma_3(k) = 3\phi_0 \lambda^2 \int_q (f(i\omega, \epsilon_{\mathbf{k}+\mathbf{q}}) - f(i\omega, -\epsilon_{\mathbf{k}+\mathbf{q}})) \gamma_y, \quad (\text{B9})$$

where we performed a partial fraction decomposition of $\frac{2\epsilon_{\mathbf{k}+\mathbf{q}}}{(i\omega + i\Omega)^2 - \epsilon_{\mathbf{k}+\mathbf{q}}^2} = \frac{1}{i\omega + i\Omega - \epsilon_{\mathbf{k}+\mathbf{q}}} - \frac{1}{i\omega + i\Omega + \epsilon_{\mathbf{k}+\mathbf{q}}}$ to arrive at the expression.

The normal part of the self energy, $\Sigma_{1,2}$ in Fig. 2(b), is contributed by the following term of the action

$$\mathcal{S}_1 = - \int_q \frac{\lambda^2}{\chi_d^{-1} \chi_N^{-1} - |\phi_0|^2} \left(\frac{\chi_d^{-1}}{4} \mathbf{S}_q \cdot \mathbf{S}_{-q} + \chi_N^{-1} \mathbf{D}_q \cdot \mathbf{D}_q^\dagger \right). \quad (\text{B10})$$

Defining $\gamma_\pm = \frac{1}{2} (\gamma_x \pm i\gamma_y)$, the corresponding contribution to the self energy is given by

$$\Sigma_1 + \Sigma_2 = \int_q \frac{\lambda^2}{M_q} \left[6 \frac{\chi_d^{-1}(q)}{4} \gamma_z G_{0,k+q} \gamma_z + 12 \chi_N^{-1}(q) (\gamma_+ G_{0,k+q} \gamma_- + \gamma_- G_{0,k+q} \gamma_+) \right] \quad (\text{B11})$$

$$= \int_{\mathbf{q}} T \sum_{i\Omega \in \text{Bosonic}} \frac{\lambda^2}{M_q} \frac{1}{(i\omega + i\Omega)^2 - \epsilon_{\mathbf{k}+\mathbf{q}}^2} \left[\frac{2}{3} (g_d - (i\Omega)^2) (i\omega + i\Omega + \epsilon_{\mathbf{k}+\mathbf{q}}\gamma_z) + 12(g_N - (i\Omega)^2)(i\omega + i\Omega - \epsilon_{\mathbf{k}+\mathbf{q}}\gamma_z) \right]. \quad (\text{B12})$$

Note that $\gamma_z G_0 \gamma_z = G_0 = i\omega - \epsilon\gamma_z$, while $\gamma_- G_0 \gamma_+ + \gamma_+ G_0 \gamma_- = i\omega + \epsilon\gamma_z$. As a result, if we consider the self energies as function of $i\omega$ and $\epsilon_{\mathbf{k}+\mathbf{q}}$, we find that $\Sigma_1 \sim \lambda^2 \int_{\mathbf{q}} \frac{3\chi_d^{-1}(q)}{2M_q} G_0(i\omega, \epsilon_{\mathbf{k}+\mathbf{q}})$ while $\Sigma_2 \sim \lambda^2 \int_{\mathbf{q}} \frac{12\chi_N^{-1}(q)}{M_q} G_0(i\omega, -\epsilon_{\mathbf{k}+\mathbf{q}})$. This allows us to argue the effect of Σ_2 pushing high energy states towards the vicinity of $\omega = 0$, while Σ_1 pushes states away from $\omega = 0$.

To perform the Matsubara sums, we define

$$h(i\omega, \epsilon, g) = T \sum_{i\Omega} \frac{-(i\Omega)^2 + g}{((i\Omega)^2 - E_+^2)((i\Omega)^2 - E_-^2)} \frac{1}{i\omega + i\Omega - \epsilon} \quad (\text{B13})$$

$$= \frac{1}{2} \frac{1}{E_+^2 - E_-^2} \left(\frac{E_+^2 - g}{E_+} (K(i\omega, \epsilon, E_+) - K(i\omega, \epsilon, -E_+)) - \frac{E_-^2 - g}{E_-} (K(i\omega, \epsilon, E_-) - K(i\omega, \epsilon, -E_-)) \right), \quad (\text{B14})$$

with $K(i\omega, \epsilon, E)$ as defined in (B8). In terms of these functions, the self energy is given by

$$\Sigma_1 = \lambda^2 \int_{\mathbf{q}} \frac{1}{3} [(h(i\omega, \epsilon_{\mathbf{k}+\mathbf{q}}, g_d) + h(i\omega, -\epsilon_{\mathbf{k}+\mathbf{q}}, g_d)) + (h(i\omega, \epsilon_{\mathbf{k}+\mathbf{q}}, g_d) - h(i\omega, -\epsilon_{\mathbf{k}+\mathbf{q}}, g_d)) \gamma_z], \quad (\text{B15})$$

$$\Sigma_2 = \lambda^2 \int_{\mathbf{q}} 6 [(h(i\omega, \epsilon_{\mathbf{k}+\mathbf{q}}, g_N) + h(i\omega, -\epsilon_{\mathbf{k}+\mathbf{q}}, g_N)) - (h(i\omega, \epsilon_{\mathbf{k}+\mathbf{q}}, g_N) - h(i\omega, -\epsilon_{\mathbf{k}+\mathbf{q}}, g_N)) \gamma_z]. \quad (\text{B16})$$

We can expand the total self energy $\Sigma = \Sigma_1 + \Sigma_2 + \Sigma_3$ in terms of Pauli matrices in Nambu space,

$$\Sigma(k) = \Sigma_{Id}(k) + \Sigma_z(k)\gamma_z + \Sigma_{\gamma_y}(k)\gamma_y, \quad (\text{B17})$$

where

$$\Sigma_{Id}(k) = \lambda^2 \int_{\mathbf{q}} \left[\frac{1}{3} (h(i\omega, \epsilon_{\mathbf{k}+\mathbf{q}}, g_d) + h(i\omega, -\epsilon_{\mathbf{k}+\mathbf{q}}, g_d)) + 6 (h(i\omega, \epsilon_{\mathbf{k}+\mathbf{q}}, g_N) + h(i\omega, -\epsilon_{\mathbf{k}+\mathbf{q}}, g_N)) \right], \quad (\text{B18})$$

$$\Sigma_z(k) = \lambda^2 \int_{\mathbf{q}} \left[\frac{1}{3} (h(i\omega, \epsilon_{\mathbf{k}+\mathbf{q}}, g_d) - h(i\omega, -\epsilon_{\mathbf{k}+\mathbf{q}}, g_d)) - 6 (h(i\omega, \epsilon_{\mathbf{k}+\mathbf{q}}, g_N) - h(i\omega, -\epsilon_{\mathbf{k}+\mathbf{q}}, g_N)) \right], \quad (\text{B19})$$

$$\Sigma_{\gamma_y}(k) = 3\phi_0 \lambda^2 \int_{\mathbf{q}} [f(i\omega, \epsilon_{\mathbf{k}+\mathbf{q}}) - f(i\omega, -\epsilon_{\mathbf{k}+\mathbf{q}})]. \quad (\text{B20})$$

Appendix C: Suppression of DOS at $\omega = 0$

In this section, we derive a compact approximate analytical expression for the suppression of the density of states (DOS) as a result of the anomalous term $\Sigma_3 = \Sigma_{\gamma_y} \gamma_y$. To this end, we focus on the limit of large bosonic velocities v_μ in χ_μ and replace the \mathbf{q} integral in Eq. (B20) with the value of the integrand at $\mathbf{q} = 0$,

$$\Sigma_{\gamma_y}(\omega + i0^+, \mathbf{k}) = 3\phi_0 \lambda^2 \frac{r_N}{v_N^2} (f(\omega + i0^+, \epsilon_{\mathbf{k}}) - f(\omega + i0^+, -\epsilon_{\mathbf{k}})). \quad (\text{C1})$$

Note that we would first need to re-parametrize the integral in terms of $\tilde{\mathbf{q}} = \mathbf{q}\sqrt{r_N}/v_N$ and then set $\tilde{\mathbf{q}} = 0$. This approximation would then be valid in the large v_d/v_N limit with this re-scaling. We then Taylor expand $f(z, \epsilon)$ with respect to ϵ, ω , at a non-zero finite T (satisfying $\epsilon \ll T \ll \sqrt[4]{r_d r_N - \phi_0^2}$). In this limit, we find the self energy to be

$$\Sigma_{\gamma_y} = \frac{3\phi_0 r_N \lambda^2}{2v_N^2 T (r_d r_N - \phi_0^2)} \epsilon_{\mathbf{k}} = \alpha \epsilon_{\mathbf{k}}. \quad (\text{C2})$$

This expression is in agreement with the result in the main text [Fig. 3(a)] which shows that as $\epsilon \rightarrow 0$, the contribution of Σ_y vanishes. With such a self-energy, the spectral function is given by

$$A(\omega) = -\frac{1}{\pi} \text{Im} \frac{\omega + i0^+}{(\omega + i0^+)^2 - (1 + \alpha^2)\epsilon_{\mathbf{k}}^2}. \quad (\text{C3})$$

A simple way to look at this, is that the band structure is simply renormalized as $\epsilon_{\mathbf{k}} \rightarrow \sqrt{1 + \alpha^2} \epsilon_{\mathbf{k}}$. This reduces the effective band mass, and thus the DOS is suppressed by a factor of $\sqrt{1 + \alpha^2}$, as stated in the main text.

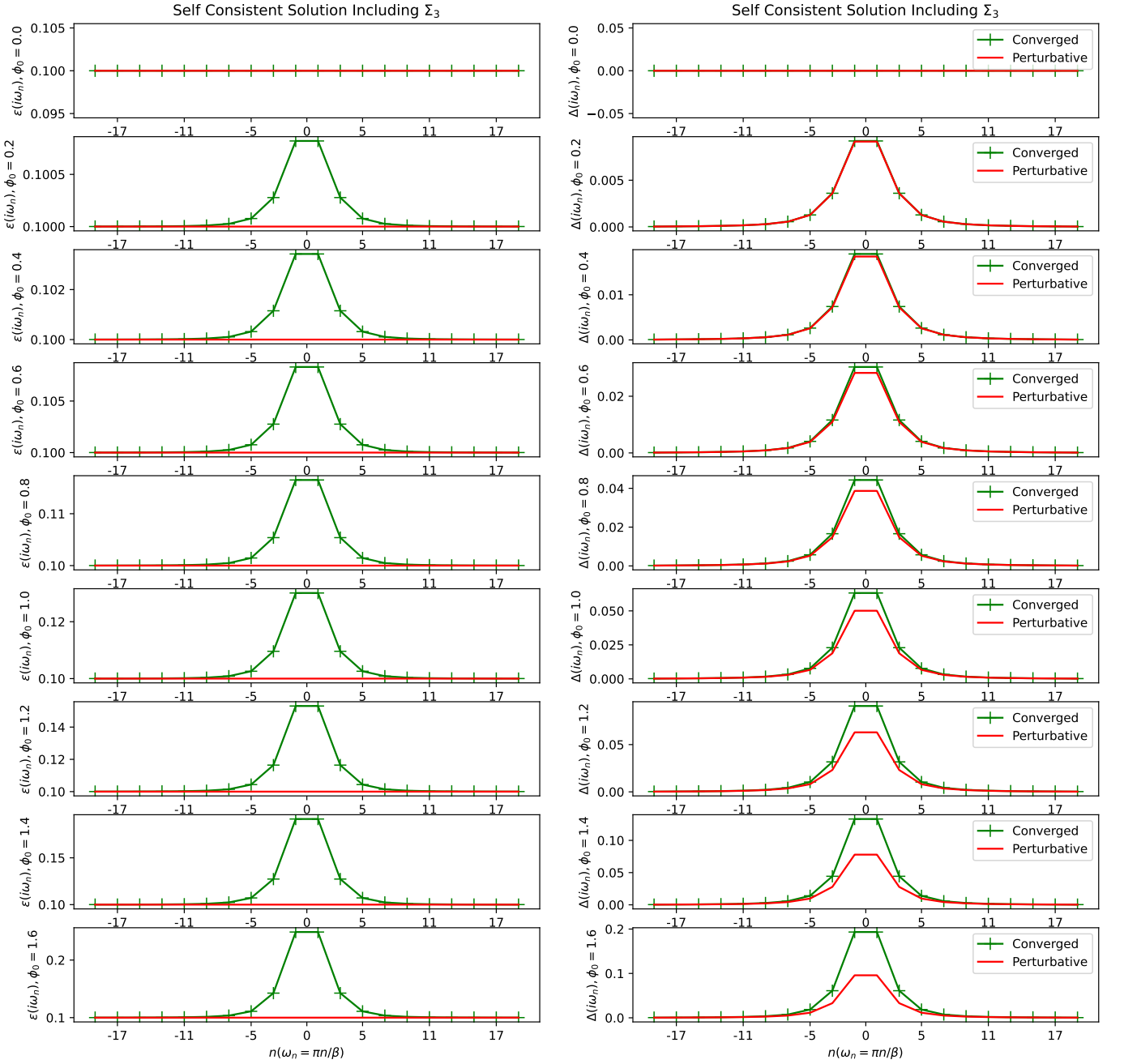


FIG. 5: The first order solution to $\varepsilon(i\omega)$, $\Delta(i\omega)$ (red) and the self consistent solution (green) for the self energy in Matsubara space. Note the offset by 0.1 in the y axis in the left column. We chose $\epsilon_{\mathbf{k}} = 0.1, r_d = 9, r_N = 1, T = \frac{1}{\beta} = 0.2, \lambda = 1$ and measured all energies in units of $\sqrt{r_N}$.

Appendix D: Higher-order corrections to electronic Green's function

In this section, we show comparisons between the first order perturbative solution and the full self consistent solution to the fermionic Green's function. We define the corrected Green's function to be $G(i\omega, \mathbf{k}) = i\omega Z_{\mathbf{k}}(i\omega) - \varepsilon_{\mathbf{k}}(i\omega)\gamma_z + \Delta_{\mathbf{k}}(i\omega)\gamma_y$. In practice, we find that $Z_{\mathbf{k}}(i\omega) \simeq 1$, so we focus on $\varepsilon_{\mathbf{k}}(i\omega)$ and $\Delta_{\mathbf{k}}(i\omega)$ in the following.

In Fig. 5, we show a comparison of the first order result for $\varepsilon_{\mathbf{k}}(i\omega_n)$ and $\Delta_{\mathbf{k}}(i\omega_n)$ after including the evaluation of the Σ_3 term of the self energy [last diagram in Fig. 2(b)] and the full self consistent solution to the self energy in Matsubara space [obtained by summing up the diagrams in Fig. 2(a) corresponding to Σ_3] at fixed \mathbf{k} . We find that for small values up to $\phi_0 \sim 0.6r_N$, the first order and self consistent solutions differ little. In first order, $\varepsilon_{\mathbf{k}}(i\omega_n)$ does

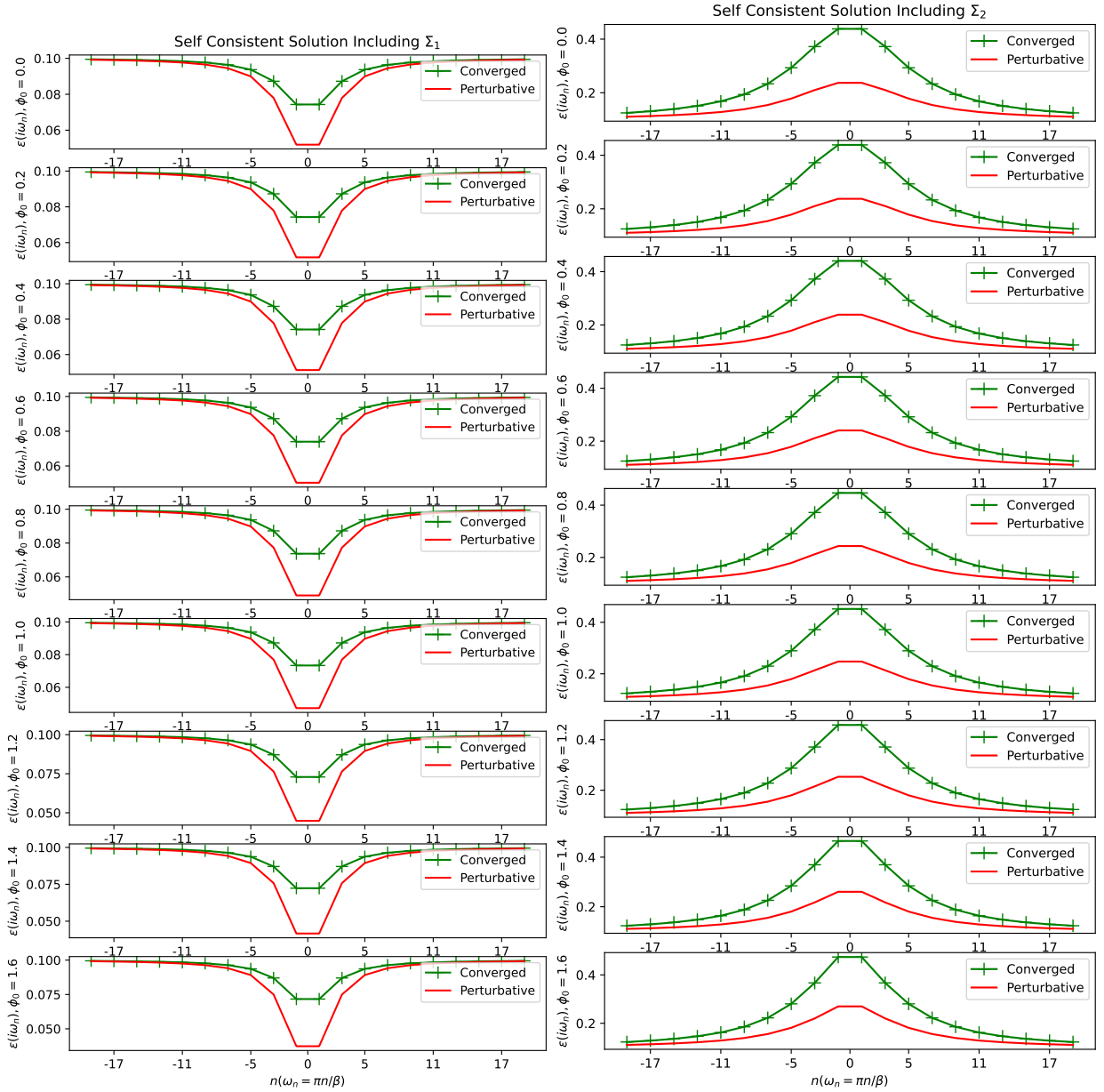


FIG. 6: The first order solution to $\varepsilon(i\omega_n)$ (red) and the self consistent solution (green) after including the effects of Σ_1 (left column) and Σ_2 (right column) separately. Same parameters as in Fig. 5.

not get renormalized since Σ_3 acquires a γ_z term only if the Green's function has a γ_y term. Such a γ_y term does not exist in the normal state about which we perform perturbation theory. As ϕ_0 increases, we find that the self consistent solution is lower in magnitude than the first order solution.

In Fig. 6, we show the corrections in $\varepsilon(i\omega_n)$ after including the effects of Σ_1 (left column) and Σ_2 (right column). As expected and argued in the main text, we find that Σ_1 and Σ_2 have qualitatively the opposite effects on the renormalization of $\varepsilon(i\omega_n)$. In both the cases, we find that the magnitude of the self consistent solution is higher than the perturbative corrections. However, since the fermionic Matsubara frequencies do not contain 0, we cannot directly say what this implies for the solution on the real axis. The magnitude of ϕ_0 has little effect on the solution since the effect of spin and triplet fluctuations are controlled by g_N and g_d , respectively, which we keep constant.

In Fig. 7, we plot the corrections in $\varepsilon(i\omega_n)$ and $\Delta(i\omega_n)$ after including the effects of all the self energies $\Sigma = \Sigma_1 + \Sigma_2 + \Sigma_3$. We find that the inclusion Σ_1 and Σ_2 together reduces the difference between the self consistent and perturbative solution (refer to the plot near $\phi_0 \sim 0$). As we increase ϕ_0 , the difference between the self consistent and perturbative solution increases due to the effect of Σ_3 which is controlled by ϕ_0 .

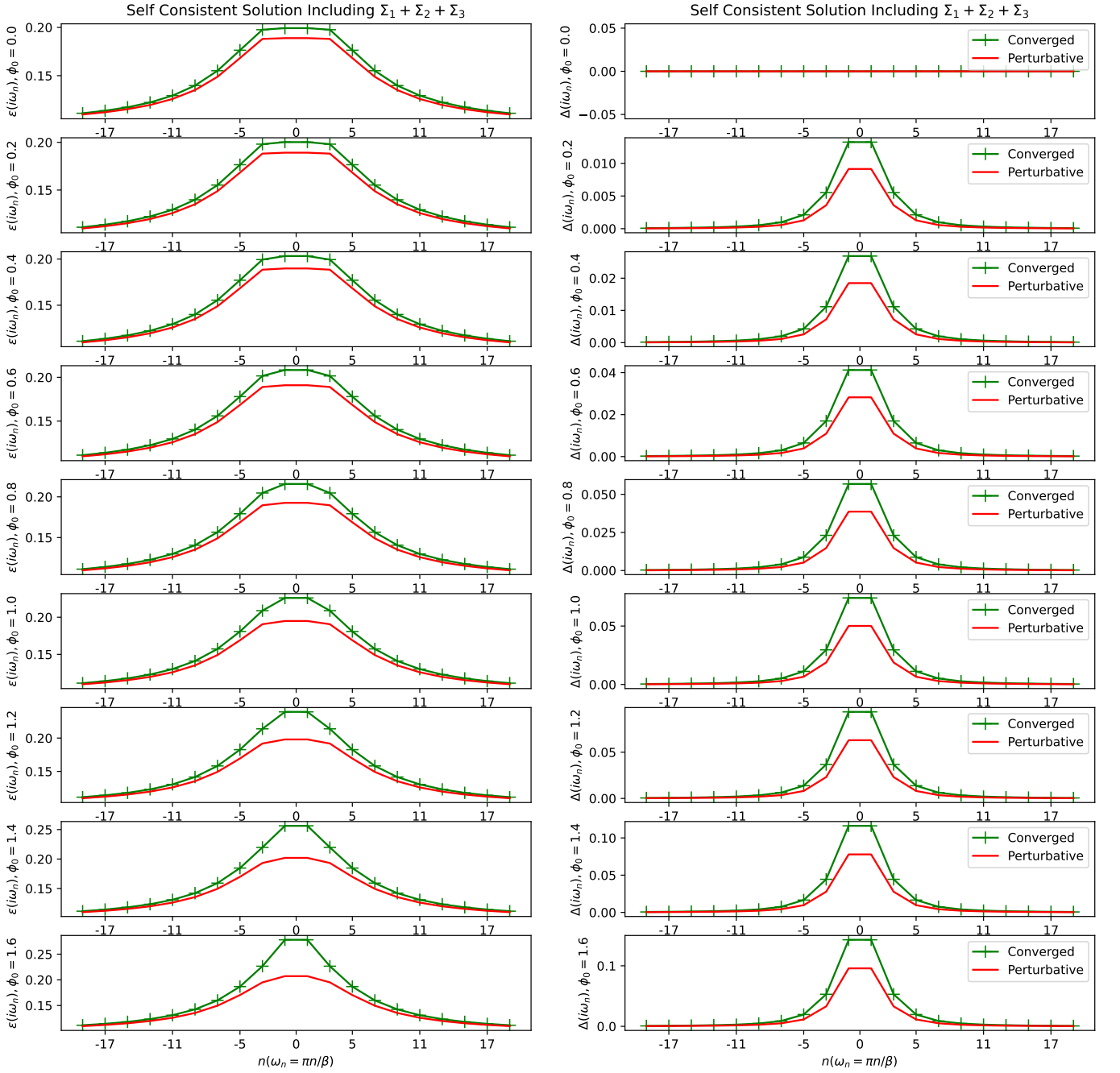


FIG. 7: The first order solution to $\varepsilon(i\omega)$, $\Delta(i\omega)$ (red) and the self consistent solution (green) after including the effects of all the terms of the self energy $\Sigma_1 + \Sigma_2 + \Sigma_3$. Same parameters as in Fig. 5.

Taken together, we see that the inclusion of second- and higher-order diagrams that contribute in the large- N limit defined in the main text yields qualitatively similar behavior on the imaginary axis compared to the first-order diagrams. We therefore expect that the qualitative picture that \mathcal{S}_1 renormalizes the DOS close to the Fermi level on top of which \mathcal{S}_2 reduces the low-energy spectral weight still applies. Since the impact of \mathcal{S}_2 is controlled by small ϕ_0 and good quantitative agreement is found for ϕ_0 up to $0.6r_N$, we expect that Fig. 3(c) would look similar when higher-order corrections were included.

Appendix E: Meissner Effect From ODLRO

The consequences of ODLRO defined in terms of four-fermion or two-boson correlators are well-known [57–60]. As a result of spin-rotation symmetry, we cannot capture ODLRO using a correlator of only two bosons. Instead, we have to study the four-boson density matrix

$$\rho(\mathbf{x}_1, \mathbf{x}_2, \mathbf{x}'_1, \mathbf{x}'_2) = \langle \mathbf{N}(\mathbf{x}_1) \cdot \mathbf{d}^*(\mathbf{x}_2) \mathbf{N}(\mathbf{x}'_1) \cdot \mathbf{d}(\mathbf{x}'_2) \rangle. \quad (\text{E1})$$

Although the derivation is in close analogy to the two-boson or four-fermion case, we here show explicitly how the Meissner effect follows from

$$\rho(\mathbf{x}_1, \mathbf{x}_2, \mathbf{x}'_1, \mathbf{x}'_2) \rightarrow \phi_0^*(\mathbf{x}_1, \mathbf{x}_2) \phi_0(\mathbf{x}'_1, \mathbf{x}'_2) \neq 0, \quad |\mathbf{x}_j - \mathbf{x}'_j| \rightarrow \infty. \quad (\text{E2})$$

Let us consider the system to be in the presence of a spatially uniform orbital magnetic field of strength $\mathbf{B} = B_0 \hat{z}$ in the out of plane direction. Note that an in-plane orbital magnetic field does not couple to the bosons as the spatial motion is constrained to the two-dimensional plane of the system. The corresponding vector potential is given by $\mathbf{A}(\mathbf{x}) = \frac{1}{2} \mathbf{B} \times \mathbf{x}$, with $\mathbf{x} = (x, y, 0)$. Under an in-plane translation by \mathbf{a} , the vector potential transforms as

$$\mathbf{A}(\mathbf{x}) \rightarrow \mathbf{A}(\mathbf{x} - \mathbf{a}) = \mathbf{A}(\mathbf{x}) - \frac{1}{2} \mathbf{B} \times \mathbf{a} \quad (\text{E3})$$

$$= \mathbf{A}(\mathbf{x}) - \frac{1}{2} \nabla [\mathbf{a} \cdot (\mathbf{x} \times \mathbf{B})] \quad (\text{E4})$$

$$= \mathbf{A}(\mathbf{x}) + \nabla \chi_{\mathbf{a}}(\mathbf{x}), \quad (\text{E5})$$

where $\chi_{\mathbf{a}}(\mathbf{x}) = -\frac{1}{2} \mathbf{a} \cdot (\mathbf{x} \times \mathbf{B})$. Note that the triplet pairing field \mathbf{d} is a charge- $2e$ bosonic field, while the magnetization field \mathbf{N} is neutral. Therefore, under simultaneous gauge transformation and displacement by \mathbf{a} in the presence of a magnetic field, the fields transform as

$$\mathbf{d}(\mathbf{x}) \rightarrow e^{i \frac{2e}{\hbar c} \chi_{\mathbf{a}}(\mathbf{x})} \mathbf{d}(\mathbf{x} - \mathbf{a}), \quad (\text{E6})$$

$$\mathbf{N}(\mathbf{x}) \rightarrow \mathbf{N}(\mathbf{x} - \mathbf{a}), \quad (\text{E7})$$

$$\mathbf{A}(\mathbf{x}) \rightarrow \mathbf{A}(\mathbf{x}). \quad (\text{E8})$$

As a result of gauge covariance and translational symmetry, the four-body density matrix obeys

$$\rho(\mathbf{x}_1, \mathbf{x}_2, \mathbf{x}'_1, \mathbf{x}'_2) = e^{i \frac{2e}{\hbar c} (\chi_{\mathbf{a}}(\mathbf{x}'_2) - \chi_{\mathbf{a}}(\mathbf{x}_2))} \rho(\mathbf{x}_1 - \mathbf{a}, \mathbf{x}_2 - \mathbf{a}, \mathbf{x}'_1 - \mathbf{a}, \mathbf{x}'_2 - \mathbf{a}). \quad (\text{E9})$$

Now suppose the system has ODLRO, i.e., Eq. (E2) holds. In combination with Eq. (E9), this implies

$$\phi_0^*(\mathbf{x}_1, \mathbf{x}_2) \phi_0(\mathbf{x}'_1, \mathbf{x}'_2) = e^{i \frac{2e}{\hbar c} (\chi_{\mathbf{a}}(\mathbf{x}'_2) - \chi_{\mathbf{a}}(\mathbf{x}_2))} \phi_0^*(\mathbf{x}_1 - \mathbf{a}, \mathbf{x}_2 - \mathbf{a}) \phi_0(\mathbf{x}'_1 - \mathbf{a}, \mathbf{x}'_2 - \mathbf{a}) \quad (\text{E10})$$

$$\implies \phi_0(\mathbf{x}_1, \mathbf{x}_2) = f_{\mathbf{a}} e^{i \frac{2e}{\hbar c} \chi_{\mathbf{a}}(\mathbf{x}_2)} \phi_0(\mathbf{x}_1 - \mathbf{a}, \mathbf{x}_2 - \mathbf{a}), \quad (\text{E11})$$

where $f_{\mathbf{a}}$ is a position-independent phase factor. Now suppose we perform two different translations by \mathbf{a} and \mathbf{b} . We can perform \mathbf{a} first and then \mathbf{b} . Alternatively, we can do \mathbf{b} first and then \mathbf{a} . They respectively give us

$$\phi_0(\mathbf{x}_1, \mathbf{x}_2) = f_{\mathbf{b}} f_{\mathbf{a}} e^{i \frac{2e}{\hbar c} \chi_{\mathbf{a}}(\mathbf{x}_2)} e^{i \frac{2e}{\hbar c} \chi_{\mathbf{b}}(\mathbf{x}_2 - \mathbf{a})} \phi_0(\mathbf{x}_1 - \mathbf{a}, \mathbf{x}_2 - \mathbf{a}), \quad (\text{E12})$$

$$\phi_0(\mathbf{x}_1, \mathbf{x}_2) = f_{\mathbf{b}} f_{\mathbf{a}} e^{i \frac{2e}{\hbar c} \chi_{\mathbf{b}}(\mathbf{x}_2)} e^{i \frac{2e}{\hbar c} \chi_{\mathbf{a}}(\mathbf{x}_2 - \mathbf{b})} \phi_0(\mathbf{x}_1 - \mathbf{a}, \mathbf{x}_2 - \mathbf{a}). \quad (\text{E13})$$

This is only consistent if

$$e^{i \frac{2e}{\hbar c} (\chi_{\mathbf{b}}(\mathbf{x}_2) + \chi_{\mathbf{a}}(\mathbf{x}_2 - \mathbf{b}) - \chi_{\mathbf{a}}(\mathbf{x}_2) - \chi_{\mathbf{b}}(\mathbf{x}_2 - \mathbf{a}))} = 1. \quad (\text{E14})$$

We can evaluate $\chi_{\mathbf{b}}(\mathbf{x}_2) + \chi_{\mathbf{a}}(\mathbf{x}_2 - \mathbf{b}) - \chi_{\mathbf{a}}(\mathbf{x}_2) - \chi_{\mathbf{b}}(\mathbf{x}_2 - \mathbf{a}) = \mathbf{B} \cdot (\mathbf{a} \times \mathbf{b})$. Thus, the condition for equality of phases becomes

$$\frac{2e}{\hbar c} \mathbf{B} \cdot (\mathbf{a} \times \mathbf{b}) = 2\pi n, \quad (\text{E15})$$

for some integer n . The only solution for arbitrary \mathbf{a}, \mathbf{b} is thus $\mathbf{B} = 0$.

Appendix F: Demonstration of Off Diagonal Long Range Order

In this section, we calculate the ODLRO wavefunctions for both the bosons and fermions. The idea is to calculate the 4–body correlator $\langle \mathbf{N}(\mathbf{x}'_1) \cdot \mathbf{d}(\mathbf{x}'_2)^* \mathbf{N}(\mathbf{x}_1) \cdot \mathbf{d}(\mathbf{x}_2) \rangle$ for the bosons and $\langle c_{\tau'_1 s'_1}^\dagger(\mathbf{x}'_1) c_{\tau'_2 s'_2}^\dagger(\mathbf{x}'_2) c_{\tau_1, s_1}(\mathbf{x}_1) c_{\tau_2, s_2}(\mathbf{x}_2) \rangle$ for the fermions. Due to the $U(1)$ symmetry breaking mediated by $\mathbf{N} \cdot \mathbf{d}$ attaining a finite expectation value (and correspondingly $c_\tau^\dagger c_{-\tau}$ for the fermions), the ODLRO factorizes into a product of functions of $\mathbf{x}_1 - \mathbf{x}_2$ and $\mathbf{x}'_1 - \mathbf{x}'_2$ in the limit $\mathbf{x} - \mathbf{x}' \rightarrow \infty$, where $\mathbf{x} = \frac{\mathbf{x}_1 + \mathbf{x}_2}{2}$ and $\mathbf{x}' = \frac{\mathbf{x}'_1 + \mathbf{x}'_2}{2}$, giving rise to ODLRO. These wavefunctions decay as a function of their respective relative coordinates $\mathbf{x}_1 - \mathbf{x}_2$ and $\mathbf{x}'_1 - \mathbf{x}'_2$. We now calculate these “macroscopic wavefunctions” explicitly for the bosonic and fermionic cases.

1. Bosonic ODLRO

The bosonic ODLRO is given by $\langle \mathbf{N}(\mathbf{x}'_1) \cdot \mathbf{d}(\mathbf{x}'_2)^* \mathbf{N}(\mathbf{x}_1) \cdot \mathbf{d}(\mathbf{x}_2) \rangle \simeq \langle \mathbf{N}(\mathbf{x}'_1) \cdot \mathbf{d}(\mathbf{x}'_2)^* \rangle \langle \mathbf{N}(\mathbf{x}_1) \cdot \mathbf{d}(\mathbf{x}_2) \rangle$ as $\mathbf{x} - \mathbf{x}' \rightarrow \infty$. All the correlators are evaluated at time $t = 0$. As discussed in the main text, to demonstrate ODLRO, it is sufficient to evaluate these correlators to first non-trivial order in the coupling constants. For bosonic ODLRO it is in fact sufficient to focus on zeroth order, i.e., neglecting the coupling to the fermions. Using the translation invariance of the system (and summing over the Matsubara frequencies $i\Omega$ since we are evaluating the correlator at time $t = 0$), we then have

$$\psi_B(\mathbf{x}) = \langle \mathbf{N}(\mathbf{x}) \cdot \mathbf{d}(\mathbf{x} = 0) \rangle = \int_{\mathbf{q}} T \sum_{i\Omega} e^{i\mathbf{q} \cdot \mathbf{x}} \langle \mathbf{N}_{-\mathbf{q}} \cdot \mathbf{d}_{\mathbf{q}} \rangle \quad (\text{F1})$$

$$= \int_{\mathbf{q}} T \sum_{i\Omega} e^{i\mathbf{q} \cdot \mathbf{x}} \frac{\phi_0}{[(i\Omega)^2 - E_+^2(\mathbf{q})][(i\Omega)^2 - E_-^2(\mathbf{q})]} \quad (\text{F2})$$

$$= \int_{\mathbf{q}} e^{i\mathbf{q} \cdot \mathbf{x}} \frac{\phi_0}{2E_+(\mathbf{q})E_-(\mathbf{q})(E_+(\mathbf{q}) + E_-(\mathbf{q}))} \quad (\text{F3})$$

$$\simeq \int_{\mathbf{q}} e^{i\mathbf{q} \cdot \mathbf{x}} \frac{\phi_0}{a + b\mathbf{q}^2} \quad (\text{F4})$$

$$= \frac{\phi_0}{b} \int_{\mathbf{q}} e^{i\mathbf{q} \cdot \sqrt{\frac{a}{b}} \mathbf{x}} \frac{1}{1 + \mathbf{q}^2} = 2\pi\phi_0 K_0 \left(\sqrt{\frac{a}{b}} |\mathbf{x}| \right) / b \quad (\text{F5})$$

$$= 2\pi\phi_0 K_0 (|\mathbf{x}|/\xi) / b, \quad (\text{F6})$$

where K_0 is the zeroth modified Bessel function of second kind. In the third line, we evaluated the Matsubara sum at $T = 0$, and in the fourth line we series expanded $2E_+(\mathbf{q})E_-(\mathbf{q})(E_+(\mathbf{q}) + E_-(\mathbf{q}))$ about $\mathbf{q} = 0$ up to quadratic order. The length scale $\xi = \sqrt{\frac{b}{a}}$ is determined by r_μ, v_μ . In the limit of $|v_N - v_d| \ll v_N + v_d$, we get

$$\xi = \frac{1}{2} \sqrt{\frac{(v_N^2 + v_d^2) \left(\sqrt{r_N r_d} - \phi_0^2 + r_N + r_d \right)}{r_N r_d - \phi_0^2}}. \quad (\text{F7})$$

In Fig. 4(b), we plot the numerical ODLRO wavefunction $\psi_B(\mathbf{x})$ with the full functional dependence on \mathbf{q} in Eq. (F3) included, and compare it with the asymptotic analytical form in Eq. (F6). We find good agreement between the numerical and analytical results.

2. Fermionic ODLRO

Similarly, we can find the fermionic ODLRO, which in real space is generically written as $\langle c_{\tau'_1 s'_1}^\dagger(\mathbf{x}'_1) c_{\tau'_2 s'_2}^\dagger(\mathbf{x}'_2) c_{\tau_1, s_1}(\mathbf{x}_1) c_{\tau_2, s_2}(\mathbf{x}_2) \rangle \sim \langle c_{\tau'_1 s'_1}^\dagger(\mathbf{x}'_1) c_{\tau'_2 s'_2}^\dagger(\mathbf{x}'_2) \rangle \langle c_{\tau_1, s_1}(\mathbf{x}_1) c_{\tau_2, s_2}(\mathbf{x}_2) \rangle$ in the limit $\mathbf{x}_j - \mathbf{x}'_j \rightarrow \infty$. Here, τ, s are the valley and spin indices respectively. To demonstrate ODLRO, we thus have to evaluate the 2–fermion correlators, which in momentum space becomes

$$(\Psi_F^*(\mathbf{x}))_{s_1, s_2} = \langle c_{\tau_1, s_1}^\dagger(\mathbf{x}, t = 0) c_{\tau_2, s_2}^\dagger(\mathbf{x} = 0, t = 0) \rangle = \int_k e^{i\mathbf{k} \cdot \mathbf{x}} \langle c_{k, \tau_1, s_1}^\dagger c_{-k, \tau_2, s_2}^\dagger \rangle. \quad (\text{F8})$$

Since the superconducting pairing takes place only between electrons between opposite valleys, we will have only $\tau_2 = -\tau_1$ giving non-zero correlators. Without loss of generality we chose $\tau_1 = +, \tau_2 = -$. Up to first order in ϕ_0 , we have

$$\langle c_{k,+s_1}^\dagger c_{-k,-s_2}^\dagger \rangle = \langle c_{k,+s_1}^\dagger c_{-k,-s_2}^\dagger \left(- \int_q \frac{1}{2} \frac{\phi_0 \lambda^2}{M_q} \mathbf{S}_q \cdot \mathbf{D}_q^\dagger \right) \rangle_0, \quad (\text{F9})$$

where $\langle \dots \rangle$ is the average with respect to the interacting and $\langle \dots \rangle_0$ with respect to the non-interacting ground state. We define $G(k) = \delta_{ss'} \delta_{\tau\tau'} G_{V,k} = \frac{\delta_{ss'} \delta_{\tau\tau'}}{i\omega_n - \epsilon_{\mathbf{k}}} = -\langle c_{s,\tau} c_{s',\tau'}^\dagger \rangle$ to be the Green's function in the fermionic basis (assuming $\epsilon_{\mathbf{k}} = \epsilon_{-\mathbf{k}}$). Equation (F9) can then be evaluated as,

$$- \frac{\phi_0 \lambda^2}{2} \int_q \frac{1}{M_q} \langle c_{k,+s_1}^\dagger c_{-k,-s_2}^\dagger (\mathbf{S}_q \cdot \mathbf{D}_q^\dagger) \rangle_0 \quad (\text{F10})$$

$$= - \frac{\phi_0 \lambda^2}{2} \int_q \frac{1}{M_q} \langle c_{k,+s_1}^\dagger c_{-k,-s_2}^\dagger \left(\sum_{k_1, k_2, p_1 = \pm, p_2 = \pm} p_1 p_2 \left(c_{k_1 + q, p_1}^\dagger \mathbf{s} c_{k_1, p_1} \right) \cdot (c_{k_2 + q, p_2} i s_y \mathbf{s} c_{-k_2, -p_2}) \right) \rangle_0 \quad (\text{F11})$$

$$= -2 \frac{\phi_0 \lambda^2}{2} \int_q \frac{1}{M_q} \langle c_{k,+s_1}^\dagger c_{-k,-s_2}^\dagger \left(\sum_{k_1, p} - (c_{-k_1, -p} i s_y \mathbf{s} (-G_{V, k_1 + q, p}) \mathbf{s} c_{k_1, p}) \right) \rangle_0 \quad (\text{F12})$$

$$= -6 \frac{\phi_0 \lambda^2}{2} \int_q \frac{1}{M_q} \langle c_{k,+s_1}^\dagger c_{-k,-s_2}^\dagger \left(\sum_{k_1, p} (c_{-k_1, -p} i s_y G_{V, k_1 + q, p} c_{k_1, p}) \right) \rangle_0 \quad (\text{F13})$$

$$= -6 \frac{\phi_0 \lambda^2}{2} \int_q \frac{1}{M_q} \langle c_{k,+s_1}^\dagger c_{-k,-s_2}^\dagger \left(\sum_{k_1} (c_{-k_1, -} i s_y G_{V, k_1 + q, +} c_{k_1, +} + c_{-k_1, +} i s_y G_{V, k_1 + q, -} c_{k_1, -}) \right) \rangle_0 \quad (\text{F14})$$

$$= -6 \frac{\phi_0 \lambda^2}{2} \int_q \frac{1}{M_q} (-(-G_{V, -k, -})(i s_y)_{s_2 s_1} G_{V, k+q, +} G_{V, k, +} + (-G_{V, k, +})(i s_y)_{s_1 s_2} G_{V, -k+q, -} G_{V, -k, -}) \quad (\text{F15})$$

$$= -6 \frac{\phi_0 \lambda^2}{2} \int_q \frac{1}{M_q} G_{V, k} G_{V, -k} (G_{V, -k+q} + G_{V, k+q}) (i s_y)_{s_2 s_1}. \quad (\text{F16})$$

We continue by calculating the Matsubara sum over $i\Omega_n$ and over $i\omega_n$ [see Eq. (F8)],

$$T^2 \sum_{i\omega_n, i\Omega_n} \frac{1}{(i\Omega_n^2 - E_+(\mathbf{q})^2)(i\Omega_n^2 - E_-(\mathbf{q})^2)} G_{V, k} G_{V, -k} (G_{V, -k+q} + G_{V, k+q}) \quad (\text{F17})$$

$$= -T^2 \sum_{i\omega_n, i\Omega} \frac{1}{(i\omega_n)^2 - \epsilon_{\mathbf{k}}^2} \frac{1}{((i\Omega_n)^2 - E_+(\mathbf{q})^2)((i\Omega_n)^2 - E_-(\mathbf{q})^2)} \left(\frac{1}{i\omega_n + i\Omega_n - \epsilon_{-\mathbf{k}+\mathbf{q}}} + \frac{1}{-i\omega_n + i\Omega_n - \epsilon_{\mathbf{k}+\mathbf{q}}} \right) \quad (\text{F18})$$

$$=: X(\epsilon_{\mathbf{k}}, \mathbf{q}). \quad (\text{F19})$$

For simplicity, we here focus on the limit where the remaining sum over \mathbf{q} in Eq. (F9) is determined by its $\mathbf{q} = 0$ component. With $E_{\pm} \equiv E_{\pm}(\mathbf{q} = 0)$ and $v_N, r_N = 1$, we have

$$\hat{X}(\epsilon) \equiv X(\epsilon, \mathbf{q} \rightarrow 0) \quad (\text{F20})$$

$$= \frac{n_f(\epsilon)^2}{2\epsilon} \left(-2 \frac{e^{\beta\epsilon}}{E_+^2 E_-^2} + \frac{2}{(E_+^2 - 4\epsilon^2)(E_-^2 - 4\epsilon^2)} + \left(\frac{2\epsilon n_B(E_+) - E_+ n_f(E_+)}{E_+(E_+^2 - E_-^2)(E_+^2 - 4\epsilon^2) n_f(E_+) n_B(2\epsilon)} + E_+ \leftrightarrow E_- \right) \right), \quad (\text{F21})$$

we can then finally write

$$\Psi_F^*(\mathbf{x}) = 3|\phi_0| \lambda^2 s_y \left(\frac{1}{V} \sum_{\mathbf{k}} e^{i\mathbf{k} \cdot \mathbf{x}} \hat{X}(\epsilon_{\mathbf{k}}) \right), \quad (\text{F22})$$

$$= \frac{3|\phi_0| \lambda^2 s_y}{2\pi} \int_0^\infty dk k J_0(\mathbf{k} \cdot \mathbf{x}) \hat{X}(\hbar^2(\mathbf{k}^2 - \mathbf{k}_F^2)/(2m)). \quad (\text{F23})$$

In the second line, we assumed $\epsilon_{\mathbf{k}} = \hbar^2(\mathbf{k}^2 - \mathbf{k}_F^2)/2m$. Using this expression, we calculate the spatial profile of the fermionic ODLRO wavefunction numerically for various values of $\epsilon_F \equiv \epsilon_{\mathbf{k}_F}$ in Fig. 4(a). Unlike the case of the bosonic ODLRO (which was exponentially decaying), the fermionic ODLRO has an oscillating component superimposed on an exponentially decaying envelope.

Appendix G: Ginzburg-Landau theory

We here calculate the Landau-Ginzburg theory for the bosonic superfluid condensate parameter to leading (zeroth) order in the fermion-boson coupling λ . To tis end, we assume that ϕ_0 is now spatially and temporally varying. This results in non-zero Fourier modes ϕ_q for $\mathbf{q}, i\Omega \neq 0$.

In momentum space, the bosonic action is generalized according to

$$\mathcal{S}_B = \int_q [\chi_N^{-1}(q) \mathbf{N}_q \cdot \mathbf{N}_{-q} + \chi_{SC}^{-1}(q) \mathbf{d}_q^* \cdot \mathbf{d}_q + (\phi_0 \mathbf{d}_q \cdot \mathbf{N}_{-q} + \text{H.c.})] \quad (\text{G1})$$

$$= \int_q \begin{pmatrix} \mathbf{N}_{-q}^T & \mathbf{d}_q^\dagger \end{pmatrix} \begin{pmatrix} \chi_N^{-1}(q) & \phi_0 \\ \phi_0 & \chi_d^{-1}(q) \end{pmatrix} \begin{pmatrix} \mathbf{N}_q \\ \mathbf{d}_q \end{pmatrix} \quad (\text{G2})$$

$$\rightarrow \int_{q,k} \begin{pmatrix} \mathbf{N}_{-q-q_2}^T & \mathbf{d}_{q+q_2}^\dagger \end{pmatrix} \begin{pmatrix} \chi_N^{-1}(q) \delta_{q_2=0} & \phi_{q_2} \\ \phi_{-q_2}^* & \chi_d^{-1}(q) \delta_{q_2=0} \end{pmatrix} \begin{pmatrix} \mathbf{N}_q \\ \mathbf{d}_q \end{pmatrix} \quad (\text{G3})$$

So after integrating out \mathbf{d} and \mathbf{N} , the effective action for ϕ reads as

$$\mathcal{S}_{\text{eff}} = \frac{1}{2} \text{Tr} \ln G^{-1}[\phi], \quad (\text{G4})$$

where

$$G^{-1}[\phi](q + q_1, q) = G_0^{-1}(q) \delta_{q_1,0} + \Gamma_{q+q_1,q} \quad (\text{G5})$$

$$G_0^{-1} = \begin{pmatrix} \chi_N^{-1}(q) & 0 \\ 0 & \chi_d^{-1}(q) \end{pmatrix} \quad (\text{G6})$$

$$\Gamma_{q+q_1,q} = \begin{pmatrix} 0 & \phi_{q_1} \\ \phi_{-q_1}^* & 0 \end{pmatrix}. \quad (\text{G7})$$

To derive the Ginzburg-Landau theory for ϕ , we expand $\text{Tr} \ln G^{-1}$ upto second order in Γ , which is equivalent to second order in ϕ . This gives us

$$S_{\text{GL}} = \text{Tr} \ln(G_0^{-1} + \Gamma) \simeq \text{Tr} G_0^{-1} + \text{Tr} G_0 \Gamma - \frac{1}{2} \text{Tr} G_0 \Gamma G_0 \Gamma \quad (\text{G8})$$

Because of the diagonal structure of G_0 , and the off diagonal structure of Γ , the linear term $\text{Tr} G_0 \Gamma$ is 0. The quadratic term becomes

$$\sum_{q',q} \text{Tr} G_0(q' + q) \Gamma(q' + q, q') G_0(q') \Gamma(q', q' + q) = \sum_{q',q} \text{Tr} \begin{pmatrix} 0 & \chi_N(q' + q) \phi_q \\ \chi_d(q' + q) \phi_{-q}^* & 0 \end{pmatrix} \begin{pmatrix} 0 & \chi_N(q') \phi_{-q} \\ \chi_d(q') \phi_q^* & 0 \end{pmatrix} \quad (\text{G9})$$

$$= \sum_{q',q} \chi_N(q' + q) \chi_d(q') \phi_q \phi_q^* + \chi_N(q') \chi_d(q' + q) \phi_{-q} \phi_{-q}^* \quad (\text{G10})$$

$$= \sum_{q',q} (\chi_N(q' + q) \chi_d(q') + \chi_N(q') \chi_d(q' - q)) \phi_q \phi_q^* \quad (\text{G11})$$

$$= \sum_{q',q} (\chi_N(q' + q) \chi_d(q') + \chi_N(q' + q) \chi_d(q')) \phi_q \phi_q^* \quad (\text{G12})$$

$$= 2 \sum_{q',q} \chi_N(q' + q) \chi_d(q') \phi_q \phi_q^* \quad (\text{G13})$$

We need to evaluate

$$\begin{aligned} \sum_{q'} \chi_N(q' + q) \chi_d(q') &= \int_{\mathbf{q}'} T \sum_{i\Omega' \in \text{Bosonic}} \left(\frac{1}{((i\Omega' + i\Omega)^2 - r_N - v_N^2(\mathbf{q}' + \mathbf{q})^2)((i\Omega')^2 - r_d - v_d^2\mathbf{q}'^2)} \right) \quad (\text{G14}) \\ &= -\frac{1}{2} \int_{\mathbf{q}'} \left(\frac{1}{\sqrt{r_N + v_N^2(\mathbf{q}' + \mathbf{q}/2)^2}} + \frac{1}{\sqrt{r_d + v_d^2(\mathbf{q}' - \mathbf{q}/2)^2}} \right) \left(\frac{1}{i\Omega^2 - \left(\sqrt{r_N + v_N^2(\mathbf{q}' + \mathbf{q}/2)^2} + \sqrt{r_d + v_d^2(\mathbf{q}' - \mathbf{q}/2)^2} \right)^2} \right). \quad (\text{G15}) \end{aligned}$$

By expanding the above expression up to second order in $i\Omega$, \mathbf{q} , we find the effective action for the ϕ field to be

$$T \sum_{i\Omega, \mathbf{q}} (r_\phi - \rho(i\Omega)^2 + v^2\mathbf{q}^2) |\phi_{(\mathbf{q}, i\Omega)}|^2 \quad (\text{G16})$$

where the coefficients are given by

$$r_\phi = - \int_{\mathbf{q}'} \frac{\pi}{\sqrt{g_d} \sqrt{g_N} (\sqrt{g_d} + \sqrt{g_N})} \quad (\text{G17})$$

$$\rho = \int_{\mathbf{q}'} \frac{\pi}{\sqrt{g_d} \sqrt{g_N} (\sqrt{g_d} + \sqrt{g_N})^3} \quad (\text{G18})$$

$$v^2 = \int_{\mathbf{q}'} \frac{\pi \left(4\mathbf{q}'^2 (\sqrt{g_d} + \sqrt{g_N}) \left(\frac{v_d^2}{g_d^{3/2}} - \frac{v_N^2}{g_N^{3/2}} \right) \left(\frac{v_N^2}{\sqrt{g_N}} - \frac{v_d^2}{\sqrt{g_d}} \right) - (\sqrt{g_d} + \sqrt{g_N})^2 \left(\frac{v_d^2(3v_d^2\mathbf{q}'^2 - 2g_d)}{g_d^{5/2}} + \frac{v_N^2(3v_N^2\mathbf{q}'^2 - 2g_N)}{g_N^{5/2}} \right) \right)}{16 (\sqrt{g_d} + \sqrt{g_N})^4} \quad (\text{G19})$$

$$- \frac{2\pi \left(\frac{1}{\sqrt{g_d}} + \frac{1}{\sqrt{g_N}} \right) \left(\frac{3\mathbf{q}'^2 (\sqrt{g_N} v_d^2 - \sqrt{g_d} v_N^2)^2}{g_d g_N} - (\sqrt{g_d} + \sqrt{g_N}) \left(\frac{v_d^2(2g_d - \mathbf{q}'^2 v_d^2)}{g_d^{3/2}} + \frac{v_N^2(2g_N - \mathbf{q}'^2 v_N^2)}{g_N^{3/2}} \right) \right)}{16 (\sqrt{g_d} + \sqrt{g_N})^4} \quad (\text{G20})$$

with $g_\mu = r_\mu + v_\mu^2 \mathbf{q}^2$. We numerically calculate the quantities r_ϕ, ρ, v^2 and plot it in Fig. 4(c,d) of the main text.

Appendix H: Self-consistent equations in special limits

In this appendix, we complement the previous analysis by studying two simple limits of the model for phase (B)—mean-field theory and the limit of zero energy-momentum transfer of the bosons. This allows us to study possible non-perturbative solutions systematically. In both cases, we find that the soft gap behavior obtained within perturbation theory is also found in these descriptions as long as T is large enough/the coupling constants, λ or ϕ_0 , are small enough.

1. Mean-field Theory

In this section, we consider the effective interaction contributed by the \mathcal{S}_2 part of the action between the electrons at time $t = 0$, in the limit where we replace the q integral with the corresponding value of the integrand at $q = 0$, and then perform a mean-field decomposition of the interaction. Defining the Bogoliubov-de Gennes basis as before, $\xi_{\mathbf{k}} = \left(c_{\mathbf{k},+} \quad i s_y c_{-\mathbf{k},-}^\dagger \right)^T$, with Pauli matrix γ_i acting on it, and $\tilde{\phi}_0 = \phi_0 \lambda^2 r_N / v_N^2$ the corresponding interaction potential is given by

$$V = -\frac{1}{2} \frac{1}{\chi_d^{-1} \chi_N^{-1} - |\phi_0|^2} \left(\tilde{\phi}_0 \mathbf{S}_{q=0} \cdot \mathbf{D}_{q=0}^\dagger + \tilde{\phi}_0^* \mathbf{D}_{q=0} \cdot \mathbf{S}_{-q=0} \right) |_{q=0} \quad (\text{H1})$$

$$= -\frac{1}{2} \frac{1}{r_N r_d - |\phi_0|^2} \int_{\mathbf{k}_1, \mathbf{k}_2} \left[-\tilde{\phi}_0 \left(c_{\mathbf{k}_1}^\dagger \mathbf{s} \tau_z c_{\mathbf{k}_1} \right) \cdot \left(c_{\mathbf{k}_2} \mathbf{s} i s_y \tau_y c_{-\mathbf{k}_2} \right) + h.c \right] \quad (\text{H2})$$

$$= -\frac{1}{r_N r_d - |\phi_0|^2} \int_{\mathbf{k}_1, \mathbf{k}_2} \left[\tilde{\phi}_0 \left(\xi_{\mathbf{k}_1}^\dagger \mathbf{s} \gamma_z \xi_{\mathbf{k}_1} \right) \cdot \left(\xi_{\mathbf{k}_2}^\dagger \mathbf{s} i \gamma_- \xi_{\mathbf{k}_2} \right) + h.c \right], \quad (\text{H3})$$

while the free Hamiltonian is given by

$$H_0 = \int_{\mathbf{k}} \xi_{\mathbf{k}}^\dagger \epsilon_{\mathbf{k}} \gamma_z \xi_{\mathbf{k}}. \quad (\text{H4})$$

We consider only the effective Hamiltonian at time $t = 0$, which is why there are no Matsubara indices.

We perform a Hartree-Fock decomposition of V , which gives us

$$V = \frac{1}{r_N r_d - |\phi_0|^2} \int_{\mathbf{k}_1, \mathbf{k}_2} \left[\tilde{\phi}_0 \left(\xi_{\mathbf{k}_1}^\dagger \mathbf{s} \gamma_z \xi_{\mathbf{k}_1} \right) \cdot \left(\xi_{\mathbf{k}_2}^\dagger \mathbf{s} i \gamma_- \xi_{\mathbf{k}_2} \right) + h.c. \right] \quad (\text{H5})$$

$$\rightarrow \frac{c}{2} \int_{\mathbf{k}} \xi_{\mathbf{k}}^\dagger (\gamma_y C_{\mathbf{k}} \gamma_z + \gamma_z C_{\mathbf{k}} \gamma_y) \xi_{\mathbf{k}}, \quad (\text{H6})$$

where $C_{\mathbf{k}} = -\langle \xi_{\mathbf{k}} \xi_{\mathbf{k}}^\dagger \rangle$, $c = 6 \frac{\tilde{\phi}_0}{r_N r_d - \phi_0^2}$, choosing a gauge with real ϕ_0 ; further take ϕ_0 to be positive such that $c > 0$. Note that this correlator is related to the Green's function G by $C_{\mathbf{k}} = T \sum_{i\omega_n} G(\mathbf{k})$. Note that all the Hartree terms vanish since we do not allow for spontaneous breaking of spin-rotation invariance (recall we study finite T in 2D). The effective 2-particle Hamiltonian is given by

$$H = \int_{\mathbf{k}} \xi_{\mathbf{k}}^\dagger \left(\epsilon_{\mathbf{k}} \gamma_z + \frac{c}{2} \gamma_y C_{\mathbf{k}} \gamma_z + \frac{c}{2} \gamma_z C_{\mathbf{k}} \gamma_y \right) \xi_{\mathbf{k}} \quad (\text{H7})$$

$$= \int_{\mathbf{k}} \xi_{\mathbf{k}}^\dagger \left[\tilde{\epsilon}_{\mathbf{k}} \gamma_z + \tilde{\Delta}_{\mathbf{k}} \gamma_y \right] \xi_{\mathbf{k}} \quad (\text{H8})$$

where $\tilde{\epsilon}_{\mathbf{k}}, \tilde{\Delta}_{\mathbf{k}}$ are the self consistent band structure and gap. Making connection with the diagrammatic self consistency relationship to be discussed below, we can foresee that the resulting self consistent equation we get will be the same as (H18) but with $\tilde{\epsilon}, \tilde{\Delta}$ replaced with the corresponding $i\omega_n$ averaged value, and the whole equation itself will be $i\omega_n$ averaged.

The correlators in terms of $\tilde{\epsilon}, \tilde{\Delta}$ are given by

$$C_{\mathbf{k}} = T \sum_{i\omega_n} \frac{1}{i\omega_n - [\tilde{\epsilon}_{\mathbf{k}} \gamma_z + \tilde{\Delta}_{\mathbf{k}} \gamma_y]} = \frac{n_f(E_{\mathbf{k}}) - n_f(-E_{\mathbf{k}})}{2E_{\mathbf{k}}} \left[\tilde{\epsilon}_{\mathbf{k}} \gamma_z + \tilde{\Delta}_{\mathbf{k}} \gamma_y \right], \quad (\text{H9})$$

where $E_{\mathbf{k}} = \sqrt{\tilde{\epsilon}_{\mathbf{k}}^2 + \tilde{\Delta}_{\mathbf{k}}^2} > 0$. Thus, using (H7), the self consistency equations become

$$\tilde{\epsilon}_{\mathbf{k}} = \epsilon_{\mathbf{k}} + c \tilde{\Delta}_{\mathbf{k}} \frac{n_f(E_{\mathbf{k}}) - n_f(-E_{\mathbf{k}})}{2E_{\mathbf{k}}} \quad (\text{H10})$$

$$\tilde{\Delta}_{\mathbf{k}} = c \tilde{\epsilon}_{\mathbf{k}} \frac{n_f(E_{\mathbf{k}}) - n_f(-E_{\mathbf{k}})}{2E_{\mathbf{k}}}. \quad (\text{H11})$$

Let us define $\beta_{\mathbf{k}} = c \frac{n_f(-E_{\mathbf{k}}) - n_f(E_{\mathbf{k}})}{2E_{\mathbf{k}}} = c \frac{\tanh(\frac{E_{\mathbf{k}}}{2T})}{2E_{\mathbf{k}}}$ and first assume $\beta_{\mathbf{k}} < 1$, which always holds as long as $T > c/4$. The self consistency equations can then be rearranged as

$$\tilde{\epsilon}_{\mathbf{k}} = \frac{1}{1 - \beta_{\mathbf{k}}^2} \epsilon_{\mathbf{k}} \quad (\text{H12a})$$

$$\tilde{\Delta}_{\mathbf{k}} = \frac{-\beta_{\mathbf{k}}}{1 - \beta_{\mathbf{k}}^2} \epsilon_{\mathbf{k}}. \quad (\text{H12b})$$

Using this, we find $E_{\mathbf{k}} = \frac{\sqrt{1 + \beta_{\mathbf{k}}^2}}{1 - \beta_{\mathbf{k}}^2} \epsilon_{\mathbf{k}}$. Note, however, that $\beta_{\mathbf{k}}$ also depends on $E_{\mathbf{k}}$ and, thus, this relation should be thought of as a self consistency equation, to be solved for $\beta_{\mathbf{k}}$ or $E_{\mathbf{k}}$.

Equations (H12) allow to derive asymptotic relations. In the limit $\epsilon_{\mathbf{k}} \rightarrow 0$, we then have $E_{\mathbf{k}} \rightarrow 0$ and $\beta_{\mathbf{k}} \rightarrow \frac{c}{4T}$, ensuring the self-consistent solutions are well controlled in the $\epsilon_{\mathbf{k}} \rightarrow 0$ regime that we are interested in. Near $\epsilon_{\mathbf{k}} = 0$ and for large $T \gg c$ ($\beta_{\mathbf{k}} \ll 1$), the renormalized spectrum is given by $E_{\mathbf{k}} = \frac{\sqrt{1 + \beta_{\mathbf{k}}^2}}{1 - \beta_{\mathbf{k}}^2} \epsilon_{\mathbf{k}} \simeq \sqrt{1 + 3\beta_{\mathbf{k}}^2} \epsilon_{\mathbf{k}} \simeq \sqrt{1 + \frac{3c^2}{16T^2}} \epsilon_{\mathbf{k}}$. The suppression of DOS is now given by

$$\frac{\rho_F(\phi_0)}{\rho_F(\phi_0 = 0)} = \frac{1}{\sqrt{1 + \alpha'^2}}, \quad \alpha' = \frac{3\sqrt{3}\phi_0\lambda^2 r_N}{2v_N^2 T (r_d r_N - \phi_0^2)},$$

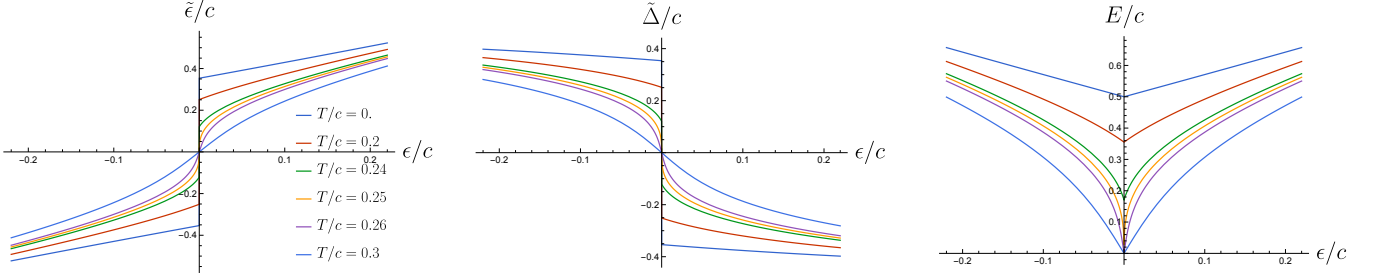


FIG. 8: The self consistent solution for $\tilde{\epsilon}_k$, $\tilde{\Delta}_k$ and E_k as a function of ϵ_k for various temperatures. At $T/c = 1/4$, the self-consistent solutions become non-analytic having an infinite slope at $\epsilon_k = 0$, and a gap opens up as the temperature decreases. There is a discontinuity in $\tilde{\epsilon}_k$, $\tilde{\Delta}_k$ at $\epsilon_k = 0$, where the gap value has different signs for $\epsilon_k \rightarrow 0^-, 0^+$.

which is of the same form as Eq. (4), found through the perturbative calculation presented in the main text and derived in Sec. C.

When $T/c = 1/4$, we have $\beta_k^2 = 1$ for $\epsilon_k \rightarrow 0$, and Eq. (H12) are not valid. At this point, the self consistent solutions open up a gap in E_k when $\epsilon_k = 0$. This gap follows by solving the equation $\beta_k^2 = 1$. When $\epsilon_k = 0$ and $\beta_k = 1$, we also have $\tilde{\epsilon}_k = -\tilde{\Delta}_k$ [see Eq. (H11)] which gives $E_k = \sqrt{2}\tilde{\epsilon}_k$. For T/c approaching $1/4$ from below, we find that $\beta_k \simeq \frac{c}{4T} \left(1 - \frac{1}{12} \frac{E_k^2}{T^2}\right)$. Thus the condition that $\beta_k^2 = 1$ gives us $E_k = \sqrt{12}T\sqrt{1 - \frac{4T}{c}}$.

To summarize, for $T > c/4$, self consistent energy and gap ($\tilde{\epsilon}$, $\tilde{\Delta}$) are proportional to ϵ . As T approaches $c/4$ from above, the slope of proportionality approaches ∞ at $\epsilon = 0$, and becomes non-analytic at $T = c/4$. Going below $T = c/4$, this non-analyticity at $\epsilon = 0$ turns into a discontinuity at $\epsilon = 0$, with the self consistent solutions developing a finite gap. The value of this gap at $T = 0$ is given as $|\tilde{\Delta}| = |\tilde{\epsilon}| = \frac{|c|}{2\sqrt{2}}$. Figure 8 illustrates the behavior obtained by numerical solution of the self-consistency equations.

2. Zero energy-momentum transfer

In this section, we consider the limit where the bosonic fields \mathbf{N}, \mathbf{d} do not transfer any momentum or Matsubara frequency in the interaction ($q = 0$ in \mathcal{S}_c). Additionally, we consider only the effect of \mathcal{S}_2 on the self energy to study the effect of the anomalous contribution. In this limit, we would like to analyze the self consistent solution of the Green's function up to all orders in λ within the large- N theory of the main text. The ansatz of the full Green's function is given by $G^{-1} = i\omega_n - \tilde{\epsilon}_k\gamma_z - \tilde{\Delta}_k\gamma_y$, since Σ_3 renormalizes only the anomalous term $\tilde{\Delta}_k$ and the spectrum $\tilde{\epsilon}_k$. We have

$$G = \frac{i\omega_n + \tilde{\epsilon}_k\gamma_z + \tilde{\Delta}_k\gamma_y}{(i\omega_n)^2 - \tilde{\epsilon}_k^2 - \tilde{\Delta}_k^2}. \quad (\text{H13})$$

Thus the self-consistent analogue of Σ_3 in Eq. (3) becomes (where we have replaced the integration over q by the $q = 0$ value of the integrand, and $\tilde{\phi}_0 = \phi_0\lambda^2 r_N/v_N^2$)

$$\Sigma_3 = 6T \frac{\tilde{\phi}_0}{r_N r_d - \phi_0^2} \frac{\tilde{\epsilon}_k\gamma_y + \tilde{\Delta}_k\gamma_z}{(i\omega_n)^2 - \tilde{\epsilon}_k^2 - \tilde{\Delta}_k^2}. \quad (\text{H14})$$

From the self-energy equation we get

$$G^{-1} = G_0^{-1} - \Sigma_3 \quad (\text{H15})$$

$$i\omega_n - \tilde{\epsilon}_k\gamma_z - \tilde{\Delta}_k\gamma_y = i\omega_n - \epsilon_k\gamma_z - 6T \frac{\tilde{\phi}_0}{r_N r_d - \phi_0^2} \frac{\tilde{\epsilon}_k\gamma_y + \tilde{\Delta}_k\gamma_z}{(i\omega_n)^2 - \tilde{\epsilon}_k^2 - \tilde{\Delta}_k^2} \quad (\text{H16})$$

$$\tilde{\epsilon}_k = \epsilon_k + Tc \frac{\tilde{\Delta}_k}{(i\omega_n)^2 - \tilde{\epsilon}_k^2 - \tilde{\Delta}_k^2} \quad (\text{H17})$$

$$\tilde{\Delta}_k = Tc \frac{\tilde{\epsilon}_k}{(i\omega_n)^2 - \tilde{\epsilon}_k^2 - \tilde{\Delta}_k^2}, \quad (\text{H18})$$

where $c = \frac{6\bar{\phi}_0}{r_N r_d - \phi_0^2}$. Right at the Fermi surface, $\epsilon_{\mathbf{k}} = 0$, the self consistency equations reduce to

$$\tilde{\epsilon}_{\mathbf{k}} = Tc \frac{\tilde{\Delta}_{\mathbf{k}}}{(i\omega_n)^2 - \tilde{\epsilon}_{\mathbf{k}}^2 - \tilde{\Delta}_{\mathbf{k}}^2} \quad (\text{H19})$$

$$\tilde{\Delta}_{\mathbf{k}} = Tc \frac{\tilde{\epsilon}_{\mathbf{k}}}{(i\omega_n)^2 - \tilde{\epsilon}_{\mathbf{k}}^2 - \tilde{\Delta}_{\mathbf{k}}^2} \quad (\text{H20})$$

$$\implies \tilde{\epsilon}_{\mathbf{k}} = T^2 c^2 \frac{\tilde{\epsilon}_{\mathbf{k}}}{(\omega_n^2 + \tilde{\epsilon}_{\mathbf{k}}^2 + \tilde{\Delta}_{\mathbf{k}}^2)^2} \quad (\text{H21})$$

There are two possible solutions to Eqs. (H19) and (H20). The first is $\tilde{\epsilon}_{\mathbf{k}} = \tilde{\Delta}_{\mathbf{k}} = 0$; this is exactly what we find within perturbation theory. For a solution with $\tilde{\epsilon}_{\mathbf{k}} \neq 0$ to exist, it must hold (assuming $\tilde{\epsilon}_{\mathbf{k}}, \tilde{\Delta}_{\mathbf{k}} \in \mathbb{R}$ as expected in the gauge that we use)

$$1 = T^2 \frac{c^2}{(\omega_n^2 + \tilde{\epsilon}_{\mathbf{k}}^2 + \tilde{\Delta}_{\mathbf{k}}^2)^2} < T^2 \frac{c^2}{\pi^4 T^4} \quad (\text{H22})$$

Thus, a non-zero solution only exists if $T < c/\pi^2 \sim c/9$. As compared to Hartree-Fock, the critical temperature for a non-perturbative solution is lower.